

Image and Object Geo-localization

Daniel Wilson^{1*}, Xiaohan Zhang¹, Waqas Sultani² and Safwan Wshah^{1*}

^{1*}Department of Computer Science, University of Vermont, Burlington, USA.

²Department of Computer Science, Information Technology University, Lahore, Pakistan.

*Corresponding author(s). E-mail(s): daniel.wilson@uvm.edu; safwan.wshah@uvm.edu;
Contributing authors: xiaohan.zhang@uvm.edu; waqas5163@gmail.com;

Abstract

The concept of geo-localization broadly refers to the process of determining an entity's geographical location, typically **in the form of** Global Positioning System (GPS) coordinates. The entity of interest may be an image, a sequence of images, a video, a satellite image, or even objects visible within the image. Recently, massive datasets of GPS-tagged media have become available due to smartphones and the internet, and deep learning has risen to prominence and enhanced the performance capabilities of machine learning models. These developments have enabled the rise of **image and object geo-localization**, which has impacted a wide range of applications such as augmented reality, robotics, self-driving vehicles, road maintenance, and 3D reconstruction. This paper provides a comprehensive survey of **visual geo-localization**, which may involve either determining the location at which an image has been captured (image geo-localization) or geolocating objects within an image (object geo-localization). We will provide an in-depth study of **visual geo-localization** including a summary of popular algorithms, a description of proposed datasets, and an analysis of performance results to illustrate the current state of the field.

Keywords: Geo-localization, Image Geo-localization, Object Geo-localization, Cross-View Geo-localization, Deep Learning

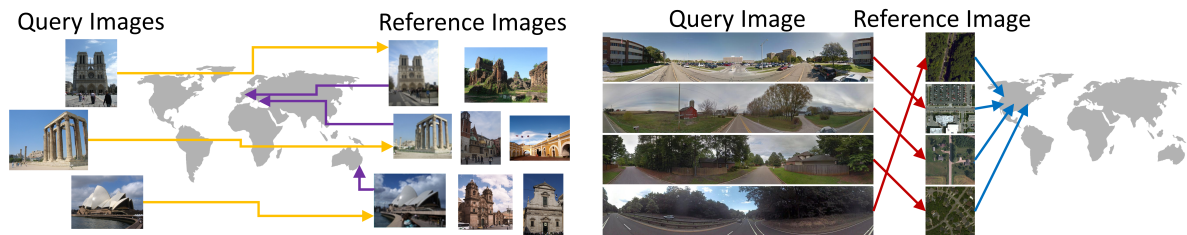
1 Introduction

Location is an important piece of context information that humans subconsciously take into account when interpreting the meaning behind a scene. For example, determining that an image is located in a popular tourist city may reveal that the image contains popular attractions, whereas a video geo-localized in a remote region may be useful to people performing land surveying. Recently, **visual geo-localization has emerged as a field in computer vision due to the richness of technical challenges it poses and its**

wide range of practical applications such as augmented reality (Middelberg, Sattler, Untzelmann, & Kobbelt, 2014), robotics (McManus, Churchill, Madern, Stewart, & Newman, 2014; Suenderhauf et al., 2015), self-driving vehicles (Chaabane, Gueguen, Trabelsi, Beveridge, & O'Hara, 2021; Suenderhauf et al., 2015), road maintenance (Chaabane et al., 2021) and 3D reconstruction (Agarwal et al., 2011).

Multiple **related fields have emerged** for extracting location information from pixel data within images. Visual geo-localization approaches, **as discussed in this paper**, specify the set of global positioning system (GPS) coordinates to which an image or objects within an image is predicted to belong. Other proposed methods involve predicting the scene depicted in an image, constructing a map of the surrounding

¹We have obtained the copyright for all figures used in this paper by purchasing all the applicable rights from their publishers.



(a) The objective of a single-view geo-localization algorithm is to determine the GPS coordinates of images without additional views. Most commonly, query images (left) are compared against reference images (right) to find a similar image with a known geo-location.

(b) Cross-view geo-localization approaches take advantage of both ground and satellite views. Ground-view query images (left) are matched to geo-tagged reference satellite images (center). The GPS locations of the reference images are used as the geo-spatial prediction (right) for the query images.

Fig. 1: Single view (left) and cross-view geo-localization (right) are the two core approaches to image geo-localization.

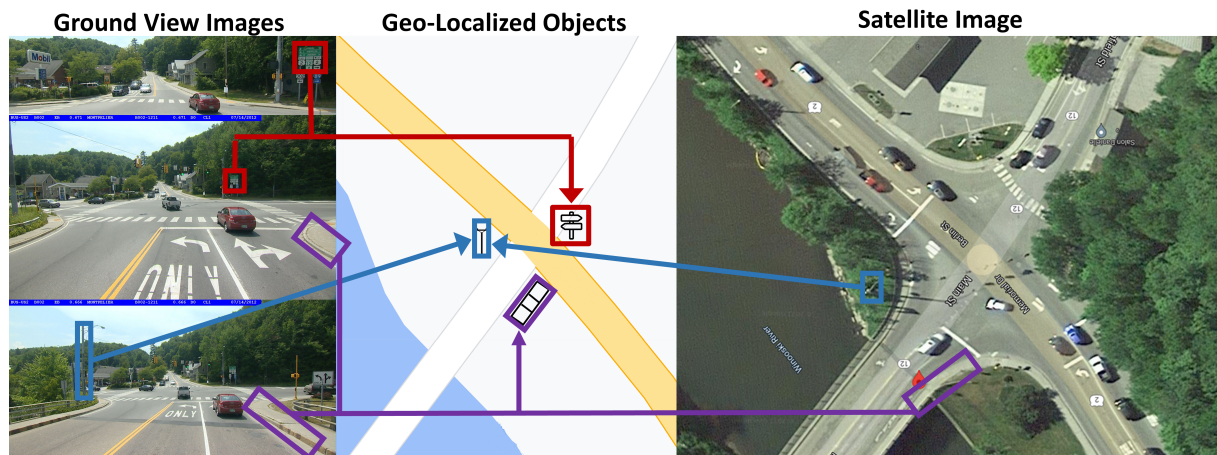


Fig. 2: A high level overview of the basic tasks performed by object geo-localization algorithms. Objects are geo-localized either from ground-view images, satellite images, or both. Note that one of the challenges associated with this task is that not all objects may be visible in both ground or satellite images.

environment, or matching the image to other similar images from a database. The source images could be taken from a variety of camera perspectives, including ground, aerial, or hybrid perspectives. Furthermore, images may depict varying environments such as city or rural settings. A detailed description of the structure of the field of visual geo-localization and its sub-fields is provided in Section 2.

In the field of visual geo-localization, few survey papers have been published. In (Brejcha & Čadík, 2017) a comprehensive study was conducted including images captured from large cities and natural environments. The authors of the paper focused mainly on non-deep learning methods as few deep learning

methods had been applied to this domain at the time this paper was published. In (Gao, Shen, Hu, & Wang, 2019) the authors conducted a comprehensive review of the state-of-the-art methods but did not provide extensive details on the existing datasets, evaluation metrics, and generative-based methods. Their survey also did not cover the emerging cross-view image geo-localization sub-field.

Our survey is the first to fully cover the breadth of the field of *visual geo-localization*, including both object and image-based approaches using ground-view, satellite-view, and cross-view images. We also place a greater emphasis on cross-view and deep-learning approaches, due to their rise to prominence

and the expectation that they will play a central role in future developments. We will present a comprehensive study of each of these sub-fields by addressing existing methods, current public datasets, and evaluation metrics. We compare each method's pros and cons and discuss their reported performance on recent public datasets. We summarize popular datasets and benchmark results in tables for accessibility and ease of readability.

The remainder of this paper is structured as follows. We will provide a high-level overview of fields related to visual geo-localization in 2. Next we will survey the three major visual geo-localization sub-categories including single-view geo-localization, cross-view geo-localization, and object geo-localization in Sections 3, 4, and 5. A visual overview of each respective geo-localization category is provided in Figure 1a, Figure 1b, and Figure 2. For each category, we will introduce the theory behind the technique, survey proposed approaches, discuss popular datasets, and describe evaluation metrics.

2 Related Fields

Computer vision-based localization algorithms have branched out into multiple intertwined sub-fields to address the unique challenges associated with different applications (see Figure 3). First, these vision-based algorithms can be broadly characterized as either *visual geo-localization* (Brejcha & Čadík, 2017; Gao et al., 2019) or *visual localization* (Piasco, Sidibé, Demonceaux, & Gouet-Brunet, 2018; Saputra, Markham, & Trigoni, 2018) approaches. These categories are distinguished based on their scale and coordinate system. *Visual localization* algorithms predict the positions of images or objects within a known spatial representation typically covering a restricted area, and are normally applied on a smaller spatial scale (Masone & Caputo, 2021; Piasco et al., 2018). Specifically, these approaches typically select a nearby object or image to use as a reference point, and predict object offsets relative to it (Piasco et al., 2018), as opposed to predicting the global position coordinates of an object. *Visual geo-localization* is concerned with determining the geospatial position of objects or images at a global scale Brejcha and Čadík (2017). Input images could originate from anywhere in the world, and thus the goal of the algorithm is to predict each image's or object's GPS coordinates. These approaches are broader in their scope due to not being

confined to a local area. The trade-off is that **the accuracy of these approaches is reduced due to their larger scale and lack of a nearby reference point to compare features against.**

Visual localization algorithms can be further divided into sub-fields. Since this paper focuses on **visual** geo-localization, we will briefly note different **visual** localization sub-fields and direct the reader to applicable survey papers for additional information. The core goal shared by all visual localization methods is to predict the relative position of objects or images within a relatively small-scale, localized environment. We direct the reader to (Masone & Caputo, 2021) and (Piasco et al., 2018) for surveys broadly focusing on image localization. One key visual localization sub-field is camera pose estimation, in which the objective is to predict the position and orientation of the camera relative to a scene or object depicted in an image. Typically, the scene or object is considered to be fixed and the camera pose variable, and thus the camera pose must be determined from each image relative to the depicted scene. An important distinction is that camera pose differs from camera position, since pose additionally includes camera x, y, and z axis rotation, whereas position exclusively refers to where a camera is located in a local coordinate system. Camera pose approaches predict the full camera pose, whereas purely image localization algorithms only predict camera position. We direct the reader to Section 4 of (Piasco et al., 2018) for additional information about camera pose estimation. Simultaneous localization and mapping (SLAM) algorithms are designed to construct maps of the surrounding environment. Like all visual localization approaches, these maps are local and not global in scale, and since they are typically applied for robot navigation, they are usually designed to run using live sensor inputs in real time. (Saputra et al., 2018) provides a survey of SLAM methods. Finally, image retrieval algorithms attempt to find images containing semantically similar objects or scenes. This task originated as a visual localization approach in which a query image must be matched to other nearby images in a local environment. As we will discuss in Section 3.1.2, image retrieval is now commonly adopted as one of the steps in **cross-view image** geo-localization pipelines. We refer the reader to (L. Zheng, Yang, & Tian, 2016) and (W. Chen et al., 2021) for an in-depth survey of this sub-field. Our survey will cover approaches that adapt image retrieval methods for **cross-view image** geo-localization.

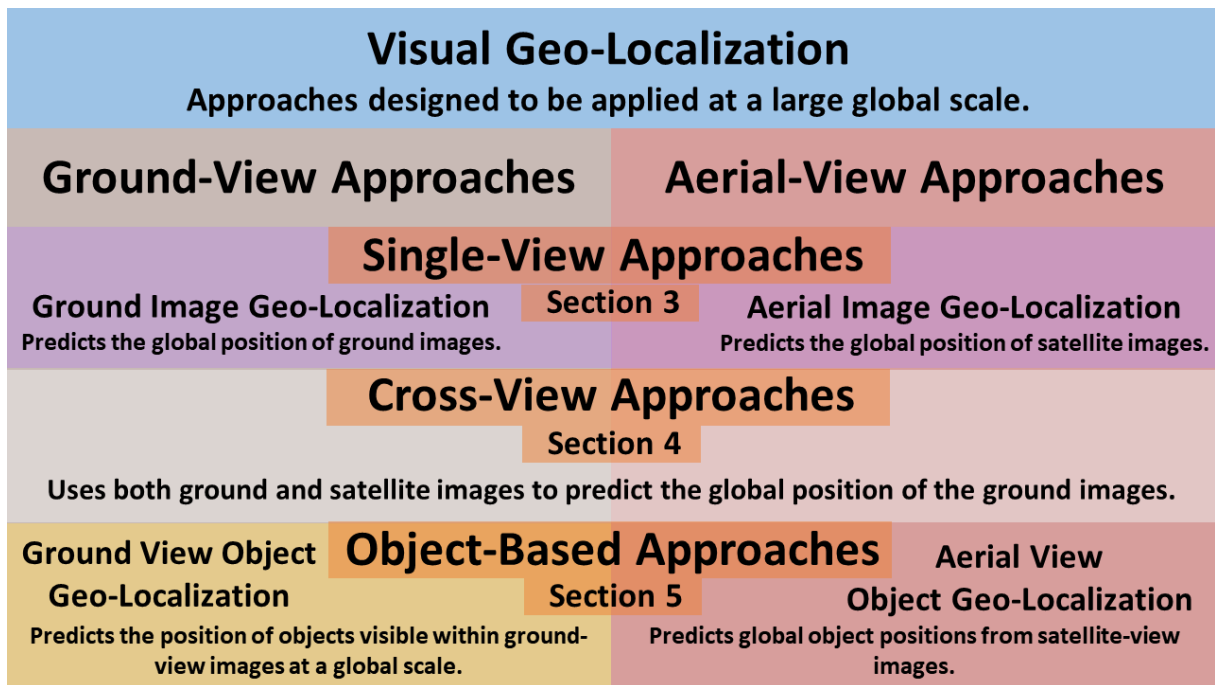


Fig. 3: Visual geo-localization, as covered in this survey, can be sub-divided based on whether the viewpoint of their input(s) are ground-view, satellite-view, or cross-view. Both ground and satellite view geo-localization may either geo-localize the position of the images, which is referred to as image geo-localization, or objects within the image, referred to as object geo-localization.

Our survey focuses on *visual geo-localization*. We remind the reader that the distinction between localization and geo-localization is that geo-localization focuses on a broader, geographical scale, where dataset images could originate from anywhere across the earth. The ultimate goal of **visual** geo-localization approaches is to predict an explicit set of GPS coordinates (Brejcha & Čadík, 2017; Gao et al., 2019), unlike localization approaches which predict positions within a local scene or relative coordinate system (Piasco et al., 2018; Saputra et al., 2018). These approaches can be divided based on whether they predict the GPS coordinates of images, referred to as *image geo-localization*, or the GPS position of objects visible within an image, referred to as *object geo-localization*. We can further divide these approaches into sub-fields based on the view perspective of the images provided to the geo-localization algorithm. *Ground-View object geo-localization* uses images taken from a ground perspective to predict the GPS coordinates and, in some cases, the class of each object visible with an image. *Satellite-View*

object geo-localization performs the same task of predicting each objects' GPS coordinates, however, the input images are from **an aerial (typically satellite)** perspective. Our paper focuses on datasets containing ground based images, so we direct the reader to Gu, Wang, and Li (2019) for an in-depth survey specifically focusing on satellite imagery. The other major sub-category of visual geo-localization approaches is *image geo-localization* algorithms, which predict the GPS coordinates of images as opposed to objects. As shown in Figure 3, *single-view geo-localization* algorithms predict the geospatial location of each image, and can be further divided into *ground-view* and *aerial-view* approaches depending on whether the input images are taken from a ground or **aerial** perspective. An interesting recent development has been the advent of *cross-view image geo-localization* approaches, which are a hybrid of ground-view and **aerial-view** image geo-localization. These methods typically employ a reference database of satellite images to identify features that can be matched to the query ground images to determine the query's geo-location. The reference image database could reach

hundreds of thousands or millions of images, yielding a complex matching problem. Since this survey covers the full field of visual geo-localization, we will cover all the approaches introduced in this paragraph.

3 Single View Image Geo-localization

Estimating the location of an image using only visual information is a uniquely challenging task as the images could be taken from anywhere in the world. The scenes depicted in images can show huge variations in time of day, weather, type of visible objects, background, and camera settings. However, images also contain useful **context** information which can help in geo-localization. This information includes landmarks, architectural details, building shapes, and surrounding environments. In single-view image geo-localization, the objective is to determine the geographic location of an image from a single camera or view. A database of reference images (also captured from the same view) may be available to assist in the geo-localization process.

This section is structured as follows. First, we introduce the main categories of techniques used to perform single-view geo-localization, followed by a description of key proposed approaches within each of these categories. Second, we describe the popular datasets commonly used for training and testing models. Finally, we discuss popular adopted benchmarks and provide a comparison of results reported by authors.

3.1 Techniques

Single view image geo-localization approaches can be broadly categorized into four main sub-categories: geographical cell-based approaches, GPS reference-based approaches, GPS refinement approaches, and **aerial-view** approaches. **Geographical cell-based geo-localization** approaches **geolocalize** images by dividing the earth into discrete geographical cells and then training a model to predict which cell an image belongs to. Since the cells could be thought of as discrete classes, these approaches are also often denoted as classification approaches. **GPS reference-based** approaches structure geo-localization as an image retrieval problem. Specifically, a large GPS-tagged image database containing images with known GPS locations is constructed. Given a query image, the GPS coordinates of the matched reference images are

used to determine the GPS coordinates of the query image. **GPS refinement** approaches are designed to refine noisy GPS coordinates (commonly found in photo albums) with the goal of increasing their accuracy. Instead of geo-localizing ground-based images, **aerial-view** approaches focus on geo-localizing aerial (such as satellite) images. Note that in contrast to cross-view geo-localization which involves jointly reasoning from both ground and aerial images, **aerial-view** approaches use aerial images only. Finally, **rural geo-localization** approaches specifically focus on predicting geographical locations of images depicting rural environments. City images are omitted from their datasets.

3.1.1 Cell-Based Image Geo-localization

A conceptually simple method of formulating image geo-localization is to structure it as a classification problem. Geographical cell-based geo-localization techniques divide Earth's geography into cells and label each GPS-tagged image with its geographical cell. A machine learning model is then trained to learn a function that maps each input image to a cell prediction. This approach has the advantage of framing the challenging geo-localization problem as a conceptually simple image classification problem, mitigating the need for an elaborate algorithm that **regresses numerical** GPS predictions. Also, since deep learning models output probabilities for each class, a model's output may still be useful to a human even if the correct cell is not assigned the greatest probability. For example, a human attempting to determine where an image was taken would still benefit if a model could narrow down its possible locations to a list of five high-probability geographical cells.

An early approach was proposed by (Zhou, Liu, et al., 2014), who built a classifier capable of predicting the city in which images were captured. Since each city is a restricted geographic location, **the cities could be loosely interpreted as representing geographical cells**. The authors employed high-level labels from the SUN database (Xiao, Hays, Ehinger, Oliva, & Torralba, 2010) to serve as scene attributes. These attributes include architecture type, water coverage, and green space. After extracting deep features for each attribute, an ensemble of Support Vector Machine (SVM) classifiers were trained to predict the attributes associated with an image and its corresponding city. At the time, this approach provided a novel idea for how to formulate geo-localization as a

Method	Type	Deep Learning vs. Traditional	Year
Im2GPS (Hays & Efros, 2008)	Reference-Based	Traditional	2008
Google Maps Localization (Zamir & Shah, 2010)	Reference-Based	Traditional	2010
Alps Skyline Segmentation (Baatz, Saurer, Köser, & Pollefeys, 2012)	Rural Geo-localization	Traditional	2012
Topographic Maps (Baatz, Saurer, Köser, & Pollefeys, 2012)	Rural Geo-localization	Traditional	2012
City Identity (Zhou, Liu, Oliva, & Torralba, 2014)	Cell-Based	Traditional	2014
Tag Refinement (Roshan Zamir, Ardeshir, & Shah, 2014)	GPS Refinement	Traditional	2014
Generalized Clique Graphs (Zamir & Shah, 2014)	Reference-Based	Traditional	2014
Skyline and Ridges (Y. Chen, Qian, Gunda, Gupta, & Shafique, 2015)	Rural Geo-localization	Traditional	2015
GPS Image Fusion (Vishal, Jawahar, & Chari, 2015)	GPS Refinement	Traditional	2015
Im2GPSv2 (Hays & Efros, 2015)	Reference-Based	Traditional	2015
View Synthesis (Torii, Arandjelović, Sivic, Okutomi, & Pajdla, 2015)	Reference-Based	Traditional	2015
Feature Prediction (H.J. Kim, Dunn, & Frahm, 2015)	Reference-Based	Traditional	2015
PlaNet (Weyand, Kostrikov, & Philbin, 2016)	Cell-Based	Deep Learning	2016
Aerial Intersections (Costea & Leordeanu, 2016)	Aerial	Traditional	2016
Feature Re-Weighting (H.J. Kim, Dunn, & Frahm, 2017)	Reference-Based	Traditional	2017
Deep Learning Era (Vo, Jacobs, & Hays, 2017)	Reference-Based	Deep Learning	2017
NetVLAD (Arandjelović, Gronat, Torii, Pajdla, & Sivic, 2018)	Reference-Based	Deep Learning	2018
CPlaNet (Seo, Weyand, Sim, & Han, 2018)	Cell-Based	Deep Learning	2018
Hierarchical Cells (Muller-Budack, Pustu-Iren, & Ewerth, 2018)	Cell-Based	Deep Learning	2018
Trip Reporting (Brejcha, Lukáč, Chen, DiVerdi, & Cadik, 2018)	Rural Geo-localization	Traditional	2018
Semantic Edges (Benbihi, Arravechia, Geist, & Pradalier, 2020)	Rural Geo-localization	Deep Learning	2020
LandscapeAR (Brejcha, Lukáč, Hold-Geoffroy, Wang, & Cadik, 2020)	Rural Geo-localization	Traditional	2020
CrossLocate (Tomešek, Čadík, & Brejcha, 2022)	Rural Geo-localization	Deep Learning	2022
Translocator (Haas, Alberti, & Skreta, 2023)	Cell-Based	Deep Learning	2023
PIGEON (Haas et al., 2023)	Cell-Based	Deep Learning	2023
Hierarchies and Scenes (Clark, Kerrigan, Kulkarni, Cepeda, & Shah, 2023)	Cell-Based	Deep Learning	2023

Table 1: Summary of single-view geo-localization methods. Each method can be characterized as either a reference-based, cell-based, rural, or GPS refinement approach. Methods can also be distinguished based on whether they apply deep learning or rely on traditional computer vision techniques.

classification problem. Compared to new approaches, however, its performance is limited by the capabilities of support vector machines and hand-crafted features, the number of cities available, and the size of the dataset.

Weyand et al. (2016) improved upon (Zhou, Liu, et al., 2014), by incorporating a deep learning model instead of relying on support vector machines. The enhanced capabilities of deep learning models enabled the authors to perform a much **larger-scale** experiment in which the surface of the earth was divided into cells. Their model was trained via standard backpropagation to predict which cell each image belonged to. The authors also studied the impact of different sized cell partitions. Since the predicted geolocation is bounded by the size of the cell, smaller sized cells are desirable to produce more accurate GPS predictions. However, reducing the cell size also results in fewer training samples per cell, **which harms performance and can cause overfitting**. (Weyand et al., 2016) proposed to satisfy both these restrictions by utilizing an adaptive partitioning in which areas more populated with images could be divided into more fine-grained cells, and areas containing fewer images would have larger cells to compensate for the lack of samples.

Later research has continued to improve cell-based geo-localization by applying improved models, developing better cell partitioning techniques, and applying larger datasets. (Seo et al., 2018) proposed to partition cells using a combinatorial approach which produces a map containing intersecting fine and coarse-grained partitions. By training separate classifiers on different cell partitionings and then aggregating the results to produce a final prediction, the authors mitigated the limitations associated with the fixed-sized cell partitioning reported in (Weyand et al., 2016).

(Muller-Budack et al., 2018) achieved further performance improvements by constructing a larger dataset and using a more sophisticated deep learning model specifically adapted to the geo-localization task. Specifically, they mined their data from Yahoo Flickr Creative Commons (Thomee et al., 2016). Each image had associated scene information indicating if its environment was indoor, natural, or urban. Their main architectural innovation was the finding that training separate classifiers for different types of scenes improved performance.

Some recent methods have been proposed to take advantage of the performance capabilities of recently popularized transformer architectures. For example, Pramanick, Nowara, Gleason, Castillo, and Chellappa

(2022) proposed Translocator, a transformer architecture which simultaneously predicts a course, middle, and fine cell partition to handle the trade-off between samples per cell and cell size. Haas et al. (2023) leveraged transformers using an agnostic geocell division approach which constructs semantically meaningful cells by applying an OPTICS Ankerst, Breunig, Kriegel, and Sander (1999) clustering algorithm. They train their transformer model, PIGEON, using a custom loss which penalizes the Haversine distance between the predicted and actual geocell. Clark et al. (2023) built a transformer architecture which used a hierarchical cross-attention method to model the relationship between different geographic levels and learn a separate representation for different environmental scenes, similar to Muller-Budack et al. (2018). While these transformer architectures are flexible computational models with the potential to yield high performance, the trade off is that they require large amounts of data, pre-training, and additional pretext tasks to reach their full potential. Pramanick et al. (2022) attempted to address this weakness by adding a second branch to their model which predicts a segmentation mask, resulting in a more robust feature representation. Haas et al. (2023) proposed a pretraining procedure in which they develop a rule-based system to create captions for their images, and then train an architecture based on the CLIP Radford et al. (2021) model to predict the captions. These pre-training tasks are intended to fine tune transformer architectures to learn domain specific features without overfitting and offset the large amounts of data these architectures require.

While cell-based approaches offer a simple framework with which to study geo-localization, these approaches suffer from an inherent limitation imposed by static cells, which is that the coordinate prediction is only as specific as the cell size. While some research has proposed improved partitioning methods, there remains an inherent trade-off between the cell size/specificity and the number of training samples. Additionally, since these methods do not employ a reference database, it is unclear if neural networks can memorize enough features to map an image from any location in the entire world to its corresponding cell.

3.1.2 Reference Based Geo-localization

The most popular approach to image geo-localization is reference-based geo-localization. These techniques localize a query image by retrieving one or more

nearby reference images with known GPS coordinates using global image features. These approaches have the advantages of being able to regress a set of GPS coordinates as opposed to restricting predictions to a single cell, and the capability to generate predictions for any location from which reference images are available.

An early reference base approach was proposed by (Hays & Efros, 2008). The authors demonstrated a baseline algorithm in which they extracted hand-crafted visual features including textures and lines, gist descriptors, and geometric context from each image. The authors computed the distance in the feature space between each query and feature image. They geo-located each query by calculating its K nearest feature spaced images and performing mean shift clustering on the geolocations of the matching images. (Hays & Efros, 2015) proposed two major improvements compared to (Hays & Efros, 2008). First, they improved the quality of extracted features by incorporating additional SIFT (Lowe, 2004) interest points using Hessian-affine and maximally stable extremely region (MSER) (Matas, Chum, Urban, & Pajdla, 2004) detectors. Second, the authors proposed an improved approach to image matching. Instead of matching images nearby in the feature space, they used a lazy learning approach inspired by SVM-KNN (H. Zhang, Berg, Maire, & Malik, 2006). This new matching algorithm yielded better performance without significantly increasing run time.

In practice, a large reference database with densely packed images will contain multiple reference images near each query, which could be further exploited for more accurate GPS predictions. Instead of matching queries to a single reference image, some works have proposed methods to match queries to multiple reference images for greater performance. (Zamir & Shah, 2010) computed SIFT descriptors and arranged them into a tree using fast approximate nearest neighbors (FLANN) (Fu, Xiang, Wang, & Cai, 2019). They proposed a GPS pruning method to remove unreliable features, and they implemented a smoothing step to handle objects which appear in multiple query images, resulting in features that were more descriptive and less redundant compared to (Hays & Efros, 2008) and (Hays & Efros, 2015). Instead of matching the query to a single reference, the authors proposed a method identifying multiple nearby reference image subsets and predicting the queries coordinates from the highest quality subsets. This produced more accurate GPS predictions than the previously proposed

methods that matched to a single reference. [Zamir and Shah \(2014\)](#) improved this approach by incorporating both local features (SIFT) and global features (GIST). Instead of matching to the first nearest neighbors, they selected the matching reference images using the NP-hard Generalized Minimum Clique Graphs (GMCP) problem. The authors benchmarked their dataset on 102,000 images that were mined from Google Street View. While approaches matching to multiple reference images make better use of the entire database by exploiting more than one matching reference image, the tradeoff is that they require a larger reference database, resulting in more computationally expensive approximate matching algorithms.

A crucial challenge faced by reference-based approaches is that the camera images will have imperfect alignments with images from the reference database. To address this fundamental challenge, some work has been proposed attempting to produce features invariant of camera perspective to make matching more robust. ([Torii et al., 2015](#)) used depth map panorama images to construct synthetic images from multiple ‘virtual’ camera locations using ray tracing and bi-linear interpolation. To match the queries to their reference database, they extracted multi-scale SIFT descriptors which were aggregated using a VLAD ([Jégou, Douze, Schmid, & Pérez, 2010](#)) descriptor followed by principal component analysis (PCA) ([Pearson, 1901](#)) and L_2 normalization. This two-stage approach is shown in Figure 5. ([D.M. Chen et al., 2011](#)) proposed a similar method using facade-aligned and viewpoint-aligned images for improved geo-localization. As shown in Figure 6, they used two parallel pipelines; one of which processed images generated from the center of the panorama (PCI), and the other used projective geometry to transform the panorama to a frontal view (PFI). A fused vocabulary representation was matched to the query image to perform geo-localization. Compared to other methods, both these approaches attempt to overcome the challenge associated with camera alignment by mining additional features from synthetic images. While this results in features that are more robust to the camera perspective, the disadvantage is that synthetic image features are less accurate than ‘real’ features from actual reference images.

To address the challenge of finding the most effective matching features, other approaches have attempted to explicitly predict how ‘useful’ a feature is, and then re-weight or remove the features based on their usefulness. ([H.J. Kim et al., 2015](#)) extracted

MSER (maximally stable extremal regions) and SIFT keypoint descriptors and proposed a per-bundle vector of locally aggregated descriptors (PBVLAD) to convert the features into a vector of fixed size. They trained an SVM to make a binary prediction indicating the ‘usefulness’ of each feature. Only features with high predicted usefulness were used to perform image matching. An important limitation of their approach was its capabilities were limited to predicting locations depicted within cities. ([H.J. Kim et al., 2017](#)) designed an end-to-end trainable convolutional network displayed in Figure 8, to compute a spatial re-weighting of features in an unsupervised manner. The intuition behind this approach is to enable the model to focus on only features relevant to the particular task. Compared to other reference-based approaches, these methods benefit from the capability to ignore less informative features, which are arguably common in large-scale geo-localization applications. The main shortcoming of these approaches is that while re-weighting reduces the impact of less useful features, it does not inherently improve the features themselves.

The rise of deep learning algorithms and their capability to automate the extraction of descriptive features posed a clear opportunity to further enhance performance. ([Vo et al., 2017](#)) extended the work of ([Hays & Efros, 2008](#)) using a modern deep learning architecture displayed in Figure 9. The authors proposed a cell-based approach in which the network simply learned to classify the query image’s cell. Second, they proposed a distance metric learning approach in which a model was trained to recognize a pair of images from nearby locations as having greater similarity. They matched the query image to similar reference images using a K-nearest neighbors. ([Arandjelović et al., 2018](#)) proposed netVLAD, a fully convolutional modification of the vector of locally aggregated descriptors (VLAD) commonly used by hand-crafted approaches. NetVLAD mimics VLAD’s pooling layer using an end-to-end trainable differentiable model optimized with a weakly supervised ranking loss. The NetVLAD architecture is displayed in Figure 10. Compared to other approaches, deep learning models have the obvious advantage of being high-performance and automating the construction of powerful feature representations. The main limitations of these approaches are the need for powerful computational hardware and large datasets required to train these CNN models.

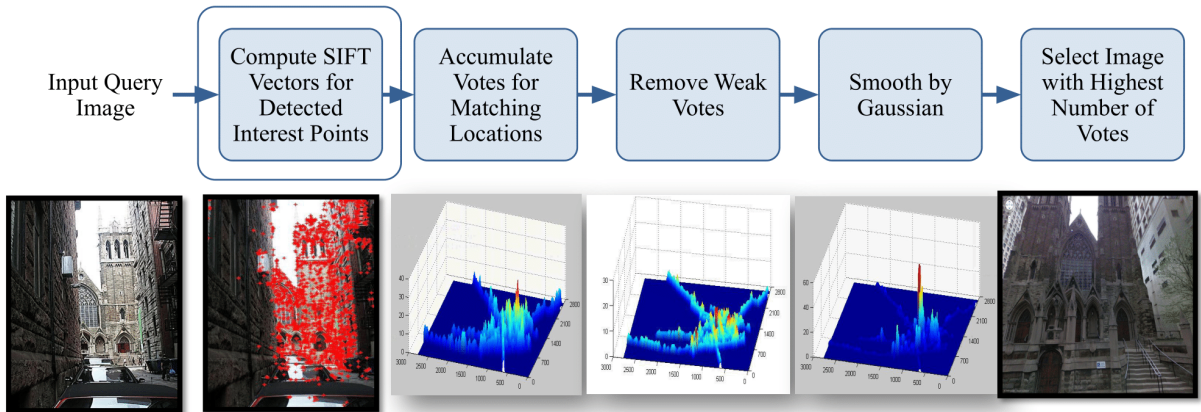


Fig. 4: A block diagram of the localization process proposed by (Zamir & Shah, 2010). SIFT vectors are calculated and used to count votes. After removing weak votes and applying a smoothing function, the reference image with the greatest number of votes is selected to predict the GPS location. Figure is taken from (Zamir & Shah, 2010).

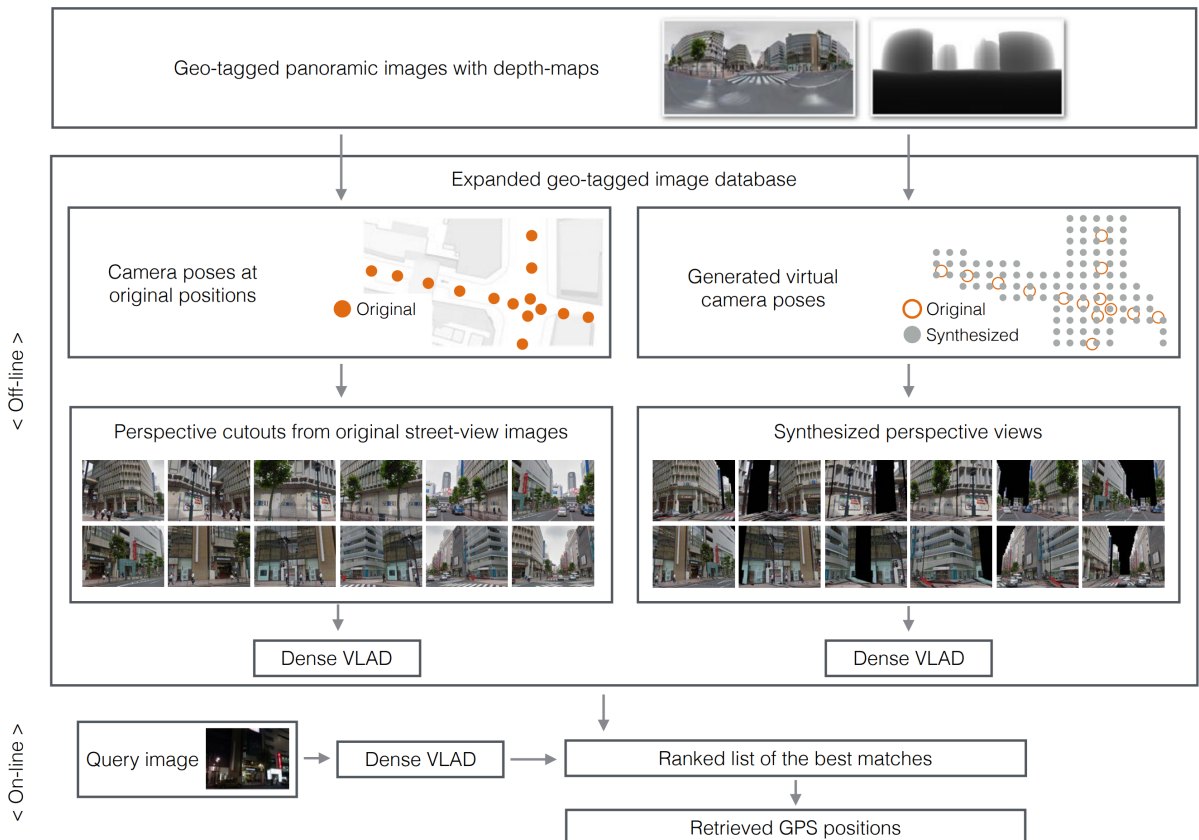


Fig. 5: An overview of the approach for place recognition proposed by (Torii et al., 2015). Their system is composed of two stages, the first of which computes features from both the original and synthesized perspective, and the second matches the query image to a similar image in the database using those features. Figure is taken from (Torii et al., 2015).

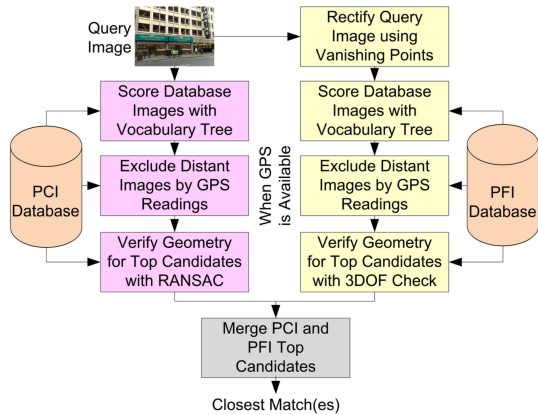


Fig. 6: The pipeline proposed by (D.M. Chen et al., 2011). The perspective central images (left) and perspective frontal images (right) are compared against separate databases in parallel. The predictions from the separate perspectives are merged to generate the candidate list to perform city-scale location recognition. Figure is taken from (D.M. Chen et al., 2011).

3.1.3 GPS Refinement Approaches

There exist many images containing inaccurate GPS coordinates due to inadequate hardware, low-quality cameras, or other sources of noise. Similarly, due to compression or storage restraints especially in photo albums, GPS information may only be available intermittently. Some researchers have proposed approaches to refine the noisy GPS locations using additional information including motion vectors between frames and extra metadata available from images.

Roshan Zamir et al. (2014) proposed an algorithm that refines GPS predictions using other images at nearby coordinates. The authors construct triplets of images with similar SIFT features containing a query image and two reference images. Structure from motion is used to compute a GPS prediction for each query image in the triplet. To reduce the noise present in the GPS tags, the authors perform random walks using an adaptive dampening factor to find subsets of data with maximal agreement. The authors constructed their dataset from user-shared images of American cities and images were downloaded from Panoramio, Flickr, and Picasa. Inspired by (Roshan Zamir et al., 2014), (Vishal et al., 2015) proposed a similar approach that also extracted SIFT features from images and performed random walks with an adaptive dampening factor to denoise GPS

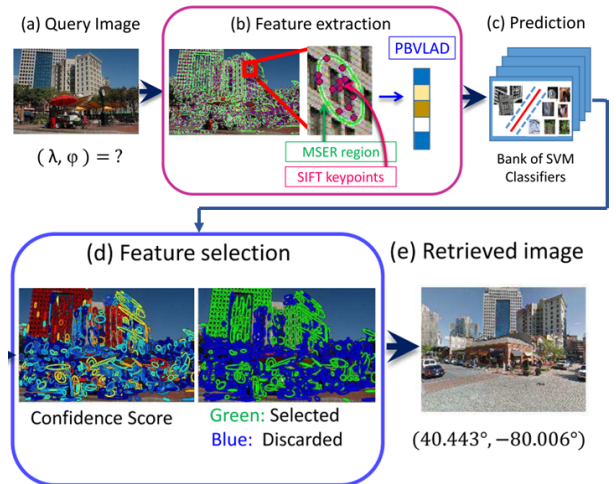


Fig. 7: An overview of the approach proposed by (H.J. Kim et al., 2015). Their pipeline extracts features from a query image, and then sends those features through SVMs which are trained to predict how useful each feature is. Only the features predicted to be useful are used for geo-localization. Figure is taken from (H.J. Kim et al., 2015).

coordinates. They further expanded the system's capabilities to geo-localize videos in order to achieve more accurate and consistent GPS signals across video frames.

Compared to other geo-localization methods, these approaches achieve superior accuracy due to refining existing GPS coordinates as opposed to predicting them from scratch. The obvious limitation of these approaches is that these techniques require noisy GPS coordinates are already present in the dataset, making their application somewhat niche.

3.1.4 Aerial-View Geo-localization Approaches

Aerial-View geo-localization algorithms attempt to regress a set of GPS coordinates for aerial images. This is in contrast to traditional reference-based image geo-localization, where the images are taken from the ground perspective. We also note that this is different from cross-view geo-localization approaches, which jointly learn from both ground and aerial images to geo-localize the ground images (Liu & Li, 2019; Regmi & Shah, 2019; Rodrigues & Tani, 2021; Tian, Chen, & Shah, 2017).

In **aerial-view** images, roads and intersections contain discriminative features, which prompted (Costea

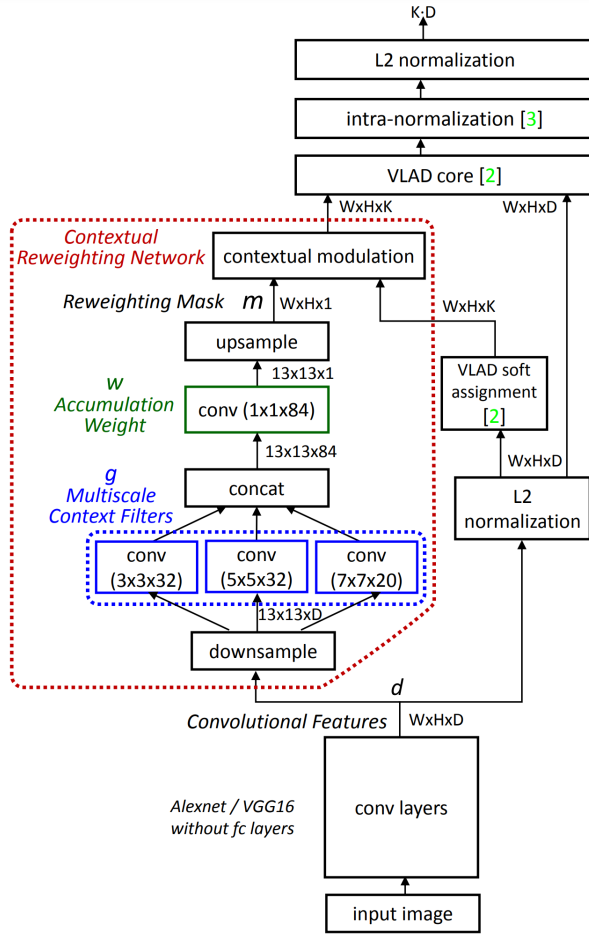


Fig. 8: The neural network architecture proposed by (H.J. Kim et al., 2017). The authors add a “contextual re-weighting network” (inside red outline) which learns to weight the relative importance of certain features based on the context of the image. Figure is taken from (H.J. Kim et al., 2017).

& Leordeanu, 2016) to propose a pipeline to perform geo-localization by matching roads and intersections against their **known locations**. The first stage of the algorithm performed image segmentation to determine road pixels in **aerial-view** images, and the second stage used the detected road pixels to identify intersections. The detected intersections were matched to known intersection locations to find the relative offset of the **aerial-view** image, from which its GPS coordinates could be calculated. The authors also constructed a geo-localization dataset containing **aerial-view** images from two European cities by collecting

ground truth information from Openstreetmap². The advantage of this approach is its capability to use intersections as a reliable feature for consistently high performance. However, an important limitation is that **aerial-view** images are less accessible than the ground-view images used by other approaches. Additionally, this method can not geo-localize images in which roads and intersections are not visible.

3.1.5 Rural Geo-Localization

The most fundamental challenge in global-scale geo-localization is that the query image could be taken from literally anywhere in the world. At many locations, photos may not contain sufficiently descriptive features for geo-localization to even be possible, such as indoor photos that don’t contain any geography-specific information. Therefore, many approaches have chosen to restrict their methodology to rural images taken from a limited area (Baatz, Saurer, Köser, & Pollefeys, 2012; Baatz, Saurer, Köser, & Pollefeys, 2012; Brejcha & Cadik, 2017).

Most early approaches were designed to exploit the fact that in contrast to city images, rural images almost always have their skyline features (mountain ranges, etc.) visible. (Baatz, Saurer, Köser, & Pollefeys, 2012; Saurer, Baatz, Köser, Ladický, & Pollefeys, 2015) used a dynamic programming algorithm to segment the skyline from images near the Alps. From the segmented skyline, they extracted contour words encoding characteristics about both the shape and order of skyline features. They employed a voting scheme to match these contourlets to the query image’s location and direction in a digital elevation model (DEM). This approach was expanded upon in (Baatz, Saurer, Köser, & Pollefeys, 2012), which used segmentation to classify each pixel from an image as being part of the sky, water, a settlement, or vegetation. The segmented images could be used to construct a textured 3D model of the surrounding terrain to assist in geo-localizing the images. (Y. Chen et al., 2015) expanded the extracted features to include ridges of the tops of hills and mountains, which provided additional features to further improve performance.

Recently proposed approaches have incorporated deep learning techniques. (Benbihi et al., 2020) utilized a CNN to extract semantic labels from each pixel in an image. They performed Canny edge detection to

²www.openstreetmap.org

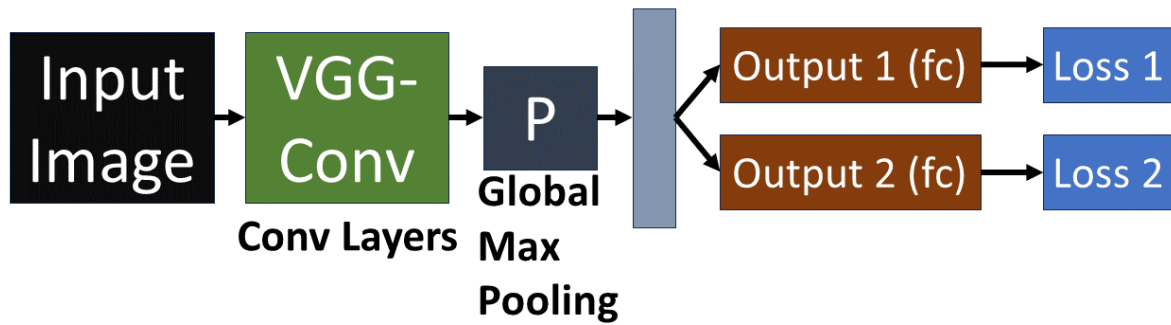


Fig. 9: The deep learning model used by Vo et al. (2017) to perform image geo-localization. The first loss penalizes the network for incorrectly classifying the cell an image belongs to, and the second loss is a ‘distance metric’ by which images less distant to each other should have more similar features. Figure is taken from (Vo et al., 2017).

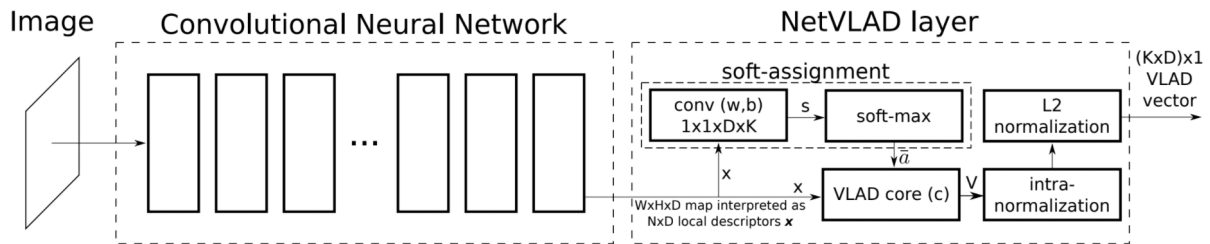


Fig. 10: A diagram showing how (Arandjelović et al., 2018) modified a traditional CNN with their proposed VLAD layer. The layer contains 1×1 convolutions followed by a softmax function which are provided as inputs to aggregate features in the “VLAD core”. Figure is taken from (Arandjelović et al., 2018).

build an edge-based wavelet-transformed image. Similar to the approaches discussed in Section 3.1.2, the images are geo-localized by comparing the Euclidean distance between features from the query image and a database of reference images. The main advantage of this approach over other proposed methods is that the extracted features are less susceptible to changes in vegetation, weather, and illumination. (Tomešek et al., 2022) employ a CNN designed to encode a feature representation for both the query and reference image. However, instead of constructing a **database of reference images**, the authors used a digital elevation model to construct synthetic reference images. This approach has the advantage of not relying on the availability of a database of reference images like many other approaches. The trade-off, however, is that synthetic reference images are unlikely to be as accurate as real reference images.

Compared to other geo-localization approaches, rural geo-localization algorithms are typically designed to operate within a more limited area, which

means they do not require sophisticated hardware like other methods. For example, (Brejcha et al., 2020) uses structure-from-motion to build a 3D model aligned to terrain from which artificial images can be rendered. The authors geo-locate the image by modeling the cross-domain feature correspondences between the rendered and query images. The full system is lightweight and can be run on a mobile device in real-time for augmented reality applications. (Brejcha et al., 2018) also uses structure from motion techniques to build a virtual digital elevation model of terrain from a sequence of images. They use embedded GPS metadata to provide a rough location, and then further align the query images using a DEM. Similarly to (Brejcha et al., 2020), their method is designed to be lightweight and can be run on weak hardware.

Rural geo-localization algorithms directly address the shortcomings of other geo-localization approaches

in rural environments where there are fewer descriptive features, primarily through the use of digital elevation models. Many of these approaches can also be run on more accessible hardware. These approaches do have many inherent limitations, however. Since all these methods rely on skyline features to some extent, they can only be applied to rural environments where these features are not blocked by man-made objects. Even in natural environments, these methods require image locations with distinguishable skylines, such as mountain ranges, to ensure the extracted features are descriptive enough to locate the images. These methods also assume the camera is positioned at a reasonably horizontal angle when calculating camera pose, however, it is generally agreed that this is a valid assumption in practice (Baatz, Saurer, Köser, & Pollefeys, 2012; Brejcha et al., 2020; Saurer et al., 2015). Perhaps the largest limitation of these approaches is that their scalability with larger geographical areas is unclear. As the locations from which these images are harvested grow, terrain and skyline features will become increasingly repeated across new locations. Future research may need to explore hybrid approaches combining multiple geo-localization methods for the best results.

3.1.6 Other Approaches

Since image geo-localization is a broad field encompassing a variety of approaches, there are many methods that are loosely related to single image geo-localization but do not decisively fit into a single category. Some of these approaches propose algorithms that involve matching queries to reference images, so a similar method could be re-used to perform reference-based geo-localization. Other approaches only perform visual localization on a smaller scale, but could potentially be scaled up to perform global localization. In this section, we briefly review some approaches that are loosely related to the field of single-image geo-localization.

(Costea & Leordeanu, 2016) proposed a pipeline to perform geo-localization by finding roads and intersections in aerial images, and then match them against their known locations. The first stage of the algorithm performs image segmentation to determine road pixels in aerial images, and the second stage uses the detected road pixels to identify intersections. The intersections were matched to known intersection locations to align the satellite image and predict its GPS location. The authors also contributed

an aerial geo-localization dataset mined from Openstreetmap³. The advantage of this approach is its high performance and interpretability compared to other methods, mainly due to the use of intersections as a reliable feature for consistent matching. However, this method cannot geo-localize images in which roads and intersections are not visible.

(Shrivastava, Malisiewicz, Gupta, & Efros, 2011) proposed a method of representing the semantic similarity between images despite how different they may be on a pixel level. This approach could be extended to perform geo-localization by applying their matching algorithm to find other nearby images with known GPS coordinates. (Kendall & Cipolla, 2016) proposed a CNN architecture and Bayesian network capable of regressing the 6-DOF (degree of freedom) camera poses of RGB images. Since their method determines pose relative to a reference point, it is comparable to geo-localization approaches except on a smaller scale.

(Hakeem, Vezzani, Shah, & Cucchiara, 2006) proposed a method of predicting the geo-spatial trajectory of a moving camera from a sequence of images extracted from a video. Part of their approach involves geo-localizing individual images similar to traditional single-image geo-localization approaches. (Kalogerakis, Vesselova, Hays, Efros, & Hertzmann, 2009) proposed a related method in which the trajectory and sequence of timestamps are used to predict the geolocation of the next image. (Agarwal et al., 2011) built a system that constructed 3D models of cities from images. Their approach extracted features for each available image within a city, detected similar features to find matching interest points, and then merged these features with a matching graph. Since their algorithm built the 3D geometry of the area, it could be extended using techniques such as (Roshan Zamir et al., 2014) to predict GPS coordinates for images.

3.2 Datasets

In this section, we will discuss popular datasets that have been collected for training and testing single-view geo-localization models. We will cover the size of each dataset, the area from which the images were taken, and any other noteworthy characteristics unique to each dataset. A summary of all the datasets is provided in Table 2.

³www.openstreetmap.org

Im2GPS:⁴ Hays and Efros (2008) built a dataset that has become a standard benchmark in the field. This dataset contains approximately 20 million images. Each image has metadata indicating the GPS coordinates at which the image was taken and geographic keywords mined from websites such as Flickr⁵. The geographic keywords are composed of terms indicating the location of the image, such as a city, state, or tourist location. The authors excluded images with tags unrelated to geolocation (concert, birthday, pets, etc.), to avoid filling the dataset with images that do not contain descriptive features for geo-localization.

Im2GPS Test:⁶ Hays and Efros (2008) also provided a small test dataset with the same structure as the training set. It contains 237 images.

Img2GPS3k:⁷ Vo et al. (2017) constructed a test set composed of 3000 images taken from the Im2GPS dataset, and hence it contains the same characteristics as described above. Due to its large size and high-quality images compared to other proposed datasets, this dataset has become accepted as a commonly used benchmark amongst researchers in the field.

City-Landmark:⁸ D.M. Chen et al. (2011) gathered data using a LIDAR (Light Detection and Ranging) system which captured 8-megapixel panoramas at 15 frames per second. The authors built a dataset containing over 150,000 GPS-tagged panoramic images in San Francisco. They aligned their panoramas with previously available 3D models of over 14,000 buildings in the city using projective geometry and LIDAR. The query images consist of GPS-tagged camera images captured by people using commonly available mobile devices, which makes this dataset especially representative of real-world applications.

KITTI:⁹ Another popular dataset in the field is contributed by Geiger, Lenz, Stiller, and Urtasun (2013). Data was captured using a road vehicle with a high-resolution camera, a GPS sensor, and a laser scanner to create ground truth labels with a high accuracy compared to other geo-localization datasets. The dataset includes varying environments including roads and highways. Unlike other geo-localization datasets, its applications are not limited to object geo-localization. Other applications include studying stereo and optical flow, visual optometry, and 3D object detection. The

authors also provided an online site for submitting and comparing performance results.

YFCC100M:¹⁰ Thomee et al. (2016) proposed the Yahoo Flickr Creative Commons (YFCC100M) dataset which contains 99.2 million images and 0.8 million videos. Each media object in the dataset contains metadata identifying the user that created it, the camera with which it was taken, and its GPS coordinates. In addition, each media object contains user-annotated tags describing what type of content it contains, such as a baby, park, etc. This dataset was not exclusively intended for image geo-localization, but due to the availability of GPS metadata, it is commonly applied to this domain.

GeoPose3k:¹¹ (Brejcha & Cadik, 2017) constructed a dataset designed for the rural geo-localization techniques discussed in Section 3.1.5. They collected over 3,000 images of the Alps from Flickr. Each image has an annotated GPS position, camera field of view, and image orientation. The dataset also provides synthetic depth maps, normal maps, illumination maps, and semantic labels for each image.

3.3 Evaluation Metrics

To quantify the performance of proposed models, consistent metrics must be adopted for measuring how accurately images are geolocated relative to their ground truth. Unfortunately, many authors have chosen to construct their own unique metrics for their specific methods and datasets, making comparisons challenging. There are, however, two standard performance metrics which have been commonly adopted and are described in this section.

Threshold Accuracy: The most universally accepted evaluation metric in this field involves defining distance thresholds and computing the percentage of images whose predicted coordinates lie within that threshold of the ground truth coordinates. Specifically, evaluation is performed using the following formula:

$$a_r = \frac{1}{N} \times \sum_{i=1}^N u[\text{geodist}(d_{gt}^i, d_{pred}^i) < r]. \quad (1)$$

In this equation, N represents the number of images during testing, r indicates the distance threshold

⁴<http://graphics.cs.cmu.edu/projects/im2gps/>

⁵<https://www.flickr.com/>

⁶<http://graphics.cs.cmu.edu/projects/im2gps/>

⁷<http://www.mediafire.com/file/7ht7sn78q27o9we/im2gps3ktest.zip/file>

⁸<http://www.nn4d.com/sanfranciscolandmark>

⁹<http://www.cvlibs.net/datasets/kitti/>

¹⁰<http://www.multimediacommons.org/>

¹¹<http://cphoto.fit.vutbr.cz/geoPose3K/>

Name	Approximate Number of Images	Locations	Special Characteristics
Im2GPS	20,000,000	Global	Images contain associated keywords
Im2GPS Test	237	Global	Im2GPS test set
Im2GPS3k	3000	Global	subset of Im2GPS dataset
City-Landmark	150,000	San Francisco	images are panoramic
KITTI	12919	Global	Designed for many other tasks such as object detection.
YFCC100M	99,200,200	Global	Images contain user annotated tags
GeoPose3k	3000	Alps	Each image has depth map, normal map, illumination map, and semantic labels.

Table 2: Summary of single view geo-localization datasets.

Im2GPS Dataset					
Method	1 km	25 km	200 km	750 km	2500 km
IM2GPS Hays and Efros (2008)	N/A	12.0	15.0	23.0	47.0
SVM-KNN Hays and Efros (2015)	2.5	21.9	32.1	35.4	71.3
PlaNet Weyand et al. (2016)	8.4	24.5	37.6	53.6	71.3
CPiNet Seo et al. (2018)	16.5	37.1	46.4	62.0	78.5
ISNs Muller-Budack et al. (2018)	16.9	43.0	51.9	66.7	80.2
Translocator Pramanick et al. (2022)	19.9	48.1	64.6	75.6	86.7
Hierarchies and Scenes Clark et al. (2023)	22.1	50.2	69.0	80.0	89.1

Table 3: The percentage of images correctly geo-localized within the specified distance threshold on the Im2GPS dataset.

within which an image is considered to be geolocalized correctly, and $u[\cdot]$ is an indicator function that returns 1 if the geo-localization threshold is less than r and 0 otherwise. Typically, this metric is reported using multiple thresholds to quantify geo-localization performance at different scales such as street, city, and country.

Reference Ranking: Another way of benchmarking performance is to list out the top ‘N’ reference images matched to the query by the geo-localization algorithm. If one or more of the top ‘N’ reference images lie within a selected threshold of the ground truth coordinates, the image is considered to be correctly geolocalized. Since this evaluation method requires comparing the query to the top N reference images, this evaluation method is only applicable to reference-based approaches. In practice, benchmarks using this metric use a threshold of 25 meters unless otherwise specified.

3.4 Benchmarks

In this section, we briefly note the experimental results of the methods discussed in Section 3.1. Benchmarks on the Im2GPS and IM2GPS3k datasets are provided in Tables 3 and 4 respectively and use the threshold accuracy evaluation metric discussed in 3.3. Benchmarks on the Tokyo 24/7 dataset are shown in 5 and use the reference ranking metric discussed in 3.3.

Im2GPS3k Dataset					
Method	1 km	25 km	200 km	750 km	2500 km
7011C Vo et al. (2017)	6.8	21.9	34.6	49.4	63.7
ISNs Muller-Budack et al. (2018)	10.5	28.0	36.6	49.7	66.0
kNN Vo et al. (2017)	12.2	33.3	44.3	57.4	71.3
Translocator Pramanick et al. (2022)	11.8	31.1	46.7	58.9	80.1
Hierarchies and Scenes Clark et al. (2023)	12.8	33.5	45.9	61.0	76.1

Table 4: The percentage of images correctly geo-localized within the specified distance threshold on the Im2GPS3k.

Tokyo 24/7 Dataset					
Method	1	5	10	20	50
Dense VLAD SYNTH Torii et al. (2015)	66.03	N/A	75.87	80.32	85.08
NetVLAD citenetvlad	68	82	87	90	N/A
CRN H.J. Kim et al. (2017)	75.2	83.8	87.3	N/A	N/A

Table 5: The performance of different methods of the Tokyo 24/7 dataset. Images are considered correctly recalled if one of the top ‘N’ listed images is within 25 meters of the ground truth. Values are expressed as percentages.

3.5 Discussion and Future Work

The fundamental goal of single-view geo-localization is to construct an algorithm that receives a single image perspective as input and predicts the image’s geographical location as output. Features are typically extracted from each image, using either a traditional hand-crafted approach or by leveraging modern deep learning architectures. These features can be either used to match the query image against a reference image, classify the image as a part of a cell, or align the image to known terrain features to perform geo-localization.

Each of the discussed methods inherits a set of trade-offs associated with its methodology. Cell-based approaches are conceptually simple because they convert the task into a simple classification problem. With modern deep learning architectures, these approaches enable the construction of a single end-to-end model which directly outputs the cell to which the query image belongs. Models constructed following this paradigm output a probability distribution of

the image corresponding to each cell, which may be useful to researchers even if the highest probability cell is not the cell the image belongs to. This simplicity comes at the expense of scalability since a suitable dataset must provide many training samples per each cell. Since training samples per cell decreases as cell size decreases, these methods are limited in their capability to perform accurate geolocalization. Since reference-based approaches match query images to a reference dataset, they can numerically regress the GPS coordinates of an image as opposed to being restricted to predicting a cell. The main disadvantage of these approaches is comparing extracted features from a query to the reference database can be computationally intensive, especially as the approach is scaled to larger databases. GPS refinement approaches produce accurate predictions with minimal effort by taking advantage of preexisting noisy GPS tags. However, they have the obvious disadvantage of requiring the image already contains geospatial information. Finally, geo-localization approaches specialized for rural environments typically predict image geolocations by aligning them to digital elevation models of the surrounding region. This formulation addresses the reduced set of features present in rural environments but comes at the expense of increased difficulty. Specifically, rural environments tend to contain fewer descriptive features, and a reference image database may be limited or completely unavailable in certain rural regions.

Previous performance improvements in this field were achieved by the extraction of more descriptive features that are better at distinguishing an image's geo-location, and are less susceptible to variations in camera perspective, vegetation, and illumination. Further progress was achieved by implementing models designed to predict the 'usefulness' of each feature to help in filtering out noise or less useful information. The largest performance improvement was achieved when deep learning models were applied to automatically extract descriptive and powerful features. The influence of larger datasets on performance should also not be overlooked. Due to the size and variety of scenery across the earth, a massive number of images is required to construct models capable of effective performance. Newer datasets have also taken careful steps to filter images that do not contain descriptive geospatial features, such as images taken indoors. Faster matching algorithms have made existing geolocalization approaches more computationally efficient.

Future performance improvements can still be achieved by incorporating additional information from datasets. For example, adding scene attributes to images that specify labels such as 'outdoor', 'concert', etc., may be beneficial to training models. This idea has received some minor exploration by (Muller-Budack et al., 2018). Certain context information available when mining data from the internet, such as the type of website they were taken from, or other images uploaded by the same user could also be used to provide additional context clues. Finally, **aerial images** of the surrounding region could serve as another reference to provide an additional perspective to a geo-localization model. Since satellite images are becoming increasingly available, their inclusion is a natural next step to further progress the state of the field. We will discuss this idea in detail in the next section.

4 Cross View Image Geo-localization

Cross-view image geo-localization approaches were developed to address the limitation of single-view approaches that at least one reference image must be near the query (Lin, Belongie, & Hays, 2013). To tackle cross-view image geo-localization, the problem is usually converted into a retrieval task by matching query ground images to reference aerial images. Note that it has become quite easy to collect dense, high-resolution geo-referenced satellite image datasets, thanks to free public releases of geo-referenced satellite images from large companies e.g., Google Earth. Although appealing, matching ground and satellite images is an extremely challenging task for several reasons: 1) satellite and ground images are most likely captured at different times resulting in different illumination conditions, weather, and objects e.g., cars and people, 2) ground and satellite views contain very different visual contents, i.e., building facades, trees, and cars occupy the majority of ground image scenes, while satellite images mainly contain building-tops, tree-tops, and road structures, 3) ground and satellite images are captured at different resolutions causing ground images to capture finer details while satellite images mainly capture coarse level information.

Applications of cross-view image geo-localization are diverse. For example, with *weak* GPS signals in metropolitan downtown areas, cross-view image geo-localization can be a supplementary source to estimate

the location of a camera (S. Zhu, Yang, & Chen, 2021b). With the development of autonomous vehicles, cross-view geo-localization can work with inertial measurement units to provide accurate positioning measurements for autonomous vehicles (D.-K. Kim & Walter, 2017). Moreover, with the recent development of Augmented Reality (AR) navigation (Dünser, Billinghamurst, Wen, Lehtinen, & Nurminen, 2012; Narzt et al., 2006; Santana, Brandao, & Sarcinelli-Filho, 2015), cross-view image geo-localization can boost the performance of AR navigation in outdoor environments.

In this section, we categorize existing cross-view image geo-localization methods into four classes: hand-crafted feature representations, graph-based feature matching, deep siamese-like methods, and generative methods. We then introduce evaluation protocols, existing datasets, and benchmark results in the cross-view image geo-localization domain.

4.1 Hand-Crafted Feature Representations

These approaches frame the cross-view geo-localization problem as a retrieval task. They extract features from aerial and ground imagery such that corresponding images from the same location should have similar features. Unlike Siamese-like CNN methods which will be discussed in later sections, these approaches rely on hand-crafted feature extractors to extract representative features from both satellite and ground images. Typically, the extracted features can be directly used for evaluating the similarity by calculating the Euclidean or Cosine distance in feature space. It can also be fed into a machine learning model, such as a support vector machine, to predict the similarity.

Feature Averaging and Discriminative Translation: Lin et al. (2013) proposed two data-driven cross-view geo-localization approaches: Data-driven Feature Averaging (AVG) and Discriminative Translation (DT). Their dataset is composed of **ground-view images**, **aerial-view images**, and land cover attribute images. Features are extracted from both ground and aerial images using four feature descriptors: HoG (Dalal & Triggs, 2005), self-similarity (Shechtman & Irani, 2007), GIST (Oliva & Torralba, 2001), and color histograms. AVG first matches the query ground view image to the top k matches in the

database using the im2gps (Hays & Efros, 2008) algorithm. Then, corresponding aerial images and land cover attribute images from the top k matches are averaged separately to build the prediction features. Finally, by matching the prediction features to the reference database, the place with the closest features is selected as the prediction result. In contrast to the AVG method which only uses the best scene matches to make predictions, the DT method takes advantage of dissimilar ground scenes. In detail, the DT method utilizes the same positive set as the AVG method and adds a negative set from the lowest match samples. A Support Vector Machine (SVM) is trained on these samples as well as on the aerial imagery. The trained SVM can be applied to predict the locations of the query ground images.

Semantic cross-view matching: Castaldo et al. (2015) leveraged a geographic information system (GIS) to perform cross-view geo-localization. Their key motivation was that the traditional feature descriptors such as SIFT (Lowe, 2004) are not useful because of the drastic appearance difference between the views. Unlike other approaches which directly compare features, they proposed to match the semantic segments to a GIS map to address the view angle difference. The ground semantic segments were obtained from an off-the-shelf algorithm (Ren, Bo, & Fox, 2012), and were transformed into a rectified view. For feature extraction, the authors proposed a Semantic Segment Layout (SSL) descriptor which is designed to simultaneously capture the semantic information and encode the rough geometric location. SSL is applied on both rectified semantic segments of the query image and the tiles of the GIS map. Finally, by matching the query features to the candidate features from the GIS map using the L_2 distance, the query images are geo-localized. Their approach is illustrated in Figure 11.

4.2 Graph-Based Methods

Graph-based cross-view image geo-localization explicitly constructs a graph according to nearby landmarks such as trees, buildings, and roads. Usually, each node in this graph represents a landmark and each edge represents the connectivity between landmarks. In this section, we present two methods that take the advantage of graphs to perform cross-view geo-localization. (Bansal & Daniilidis, 2014) leveraged dense buildings in urban areas and (Verde,

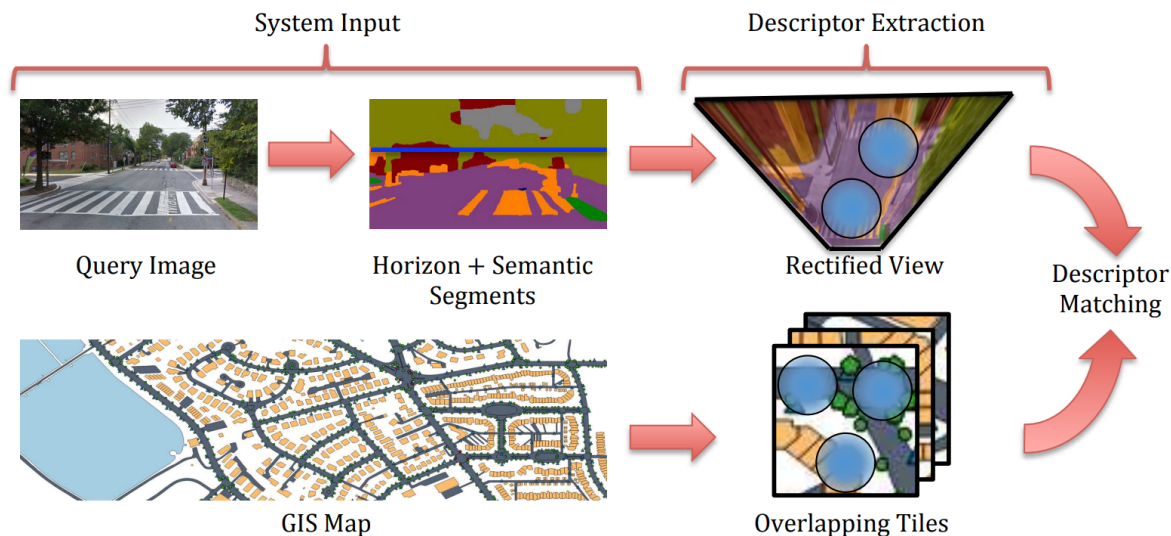


Fig. 11: Pipeline of Semantic cross-view matching. The descriptors extract features from both the query input stack (image and segments) and the tiled GIS map. The estimated location is the GIS tile that is closest to the query image in L_2 distance. Figure is taken from (Castaldo et al., 2015).

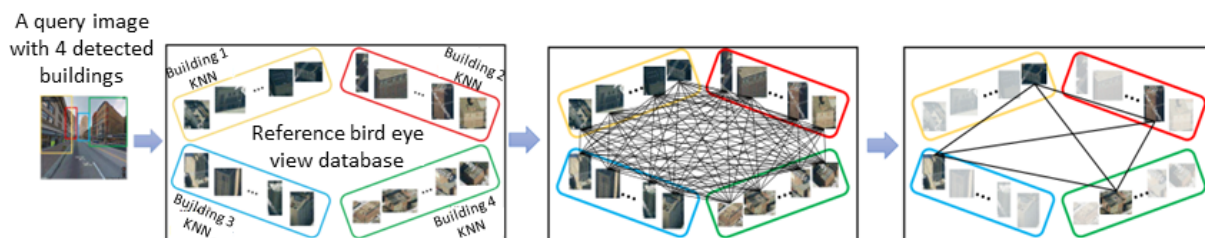


Fig. 12: Visualization of the cross-view image geo-localization approach from (Tian et al., 2017). First all buildings are detected from the query image. Then a building matching model retrieves K nearest neighbors' aerial-view buildings in latent space. Finally, it performs building matching using dominant sets and estimates the location of the query image. The image is taken from (Tian et al., 2017).

Resek, Milani, & Rocha, 2020) utilized the relative location of pre-annotated landmarks. Since landmarks are *explicitly* modeled in the graph, the matching result can be easily explained by the correspondence between the two views. Thus, graph-based cross-view geo-localization naturally has better interpretability than other methods introduced in this section.

Building matching: Tian et al. (2017) proposed to match the surrounding buildings in two views to geo-localize in urban areas. The proposed pipeline has five stages: building detection from both overhead and ground images, building matching between cross-view images, retrieval of the nearest k neighbors

for each building, dominant set selection, and geo-localization. To detect buildings from ground images, a Fast R-CNN model (Girshick, 2015) is employed. For each detected building, a siamese (Chopra, Hadsell, & LeCun, 2005) building matching network predicts the relevance between the building and other buildings detected from overhead images. This network is trained using a contrastive loss (Hadsell, Chopra, & LeCun, 2006) on a dataset customized for building matching. For each building, the top k nearest neighbors are then selected from a reference database as a cluster. After that, a graph is constructed in which the nodes are buildings and the edges are connected between buildings from different clusters.

The weight of each edge is determined by a combination of similarity scores from building matching and the physical distance. The goal is to select one reference building from each cluster, such that the total weight is maximized. The authors employ a replicator dynamics algorithm (Pavan & Pelillo, 2003, 2007) to select a dominant set as shown in Figure 12. The final prediction of the geo-localization is the average of each selected building's GPS in the dominant set. A diagram of their approach is shown in Figure 12.

Landmark matching: Verde et al. (2020) proposed a graph matching method that assumed the location of the buildings, roads, and trees were pre-annotated on a map. The key idea was to construct co-visibility matrices from the locations of the pre-annotated landmarks to represent the adjacency from both satellite view and ground view. Candidate locations were extracted by identifying the regions in which the query and reference matrices overlapped. Then, a class adjacent matrix was built by calculating the edge type for each candidate matrix and query matrix. Finally, a Bayesian-based posterior maximum algorithm was adopted for selecting the closest matching satellite image for geo-localization. Compared with matching only buildings (Tian et al., 2017), landmark matching (Verde et al., 2020) includes more classes of objects such as trees and roads. However, this paper assumed that the availability of pre-annotated landmarks which are not always available in real-world settings.

4.3 Deep Siamese-Like Methods

With the development of CNNs (Krizhevsky, Sutskever, & Hinton, 2012; Lecun, Bottou, Bengio, & Haffner, 1998) and siamese networks (Bromley et al., 1993; Chopra et al., 2005; Hadsell et al., 2006), deep siamese-like networks have become mainstream in cross-view image geo-localization. Similar to hand-crafted feature representation methods, siamese-like deep learning methods frame the cross-view geo-localization problem as a retrieval task. Siamese networks traditionally contain two symmetric subnetworks which share the same weights in each layer. However, in cross-view geo-localization, applying the same feature extractor to both aerial and ground perspectives may not achieve good results (Hu, Feng, Nguyen, & Lee, 2018). Recent research has demonstrated that deep siamese-like methods which jointly

train the two subnetworks with unique weights outperform the traditional siamese network in which the weights are shared. Thus, the model can learn a more domain-specific feature representation than the hand-crafted feature extractor and achieve more competitive results.

Where-CNN: Lin, Cui, Belongie, and Hays (2015) proposed Where-CNN which is the first CNN model to address cross-view image geo-localization using a siamese network (Chopra et al., 2005). Unlike most of the methods described in this section which geo-localized the given street view images from aerial images, this paper proposed to use reference images from an oblique aerial view (bird's eye view). The key idea of this approach is that oblique aerial images share more common features with ground-level images than satellite images. To achieve this goal, the two branches of Where-CNN were modified from an AlexNet (Krizhevsky et al., 2012) which was pre-trained on the ImageNet (Deng et al., 2009) and Places (Zhou, Lapedriza, Xiao, Torralba, & Oliva, 2014) datasets. Features extracted from the last fully connected layer were normalized to have a zero mean and unit standard deviation. A contrastive loss (Hadsell et al., 2006) was applied for fine-tuning the model.

MCVPlaces: Workman, Souvenir, and Jacobs (2015) proposed the MCVPlaces model which was the first Siamese-like CNN model that performed cross-view geo-localization on *satellite* and ground-level images. MCVPlaces contained a multi-scale aerial feature extractor and a ground-level image feature extractor which was pre-trained on the Places (Zhou, Lapedriza, et al., 2014) dataset. The authors proposed to only optimize the satellite feature extractor during the training phase and freeze the ground-level image feature extractor. A large-scale cross-view dataset, Crossview USA (CVUSA) was proposed and used to train the MCVPlaces model with a Euclidean distance loss on ground and satellite features. The CVUSA dataset was later refined in (Zhai, Bessinger, Workman, & Jacobs, 2017) and became one of the most popular datasets in the cross-view geo-localization field.

DBL: Vo and Hays (2016) explored the effectiveness of four different architectures including classification architectures, hybrid Siamese-classification architectures, Siamese architectures, and triplet architectures,

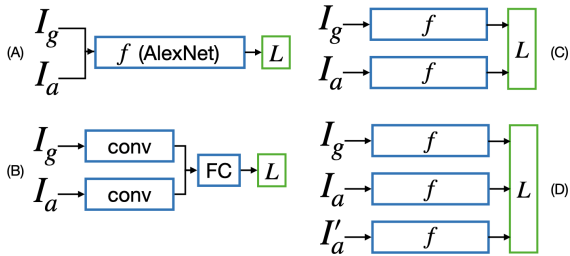


Fig. 13: Four different structures are explored in (Vo & Hays, 2016). I_g represents the ground image. I_a is the aerial image. I'_a is the negative aerial image from the triplet model. (a) indicates a classification model, (b) is a hybrid siamese-classification model, (c) is a siamese model, and (d) is a triplet model

as shown in Figure 13. A novel Distance-Based Logistic (DBL) loss layer was proposed for training the models. To evaluate the performance of the different architectures, the authors collected a large-scale dataset. Crucially, the goal of this paper was to localize the scenes depicted in the photo which is different compared to other methods in this section that geo-localize the location of the camera. The authors concluded that the triplet network achieved the best results on the testing set. Furthermore, an exhaustive mini-batch strategy was proposed in this paper to obtain maximum negative samples for a ground truth pair. In detail, assuming M sampled locations in a mini-batch, each location has a ground-satellite pair. To construct triplet pairs for training, each query ground image has to have 1 positive reference satellite image (ground truth) and $M - 1$ negative reference satellite images. Similarly, each query satellite image has to have 1 positive reference ground image (ground truth) and $M - 1$ negative reference ground images. Thus, in this mini-batch, a total of $M \times 2(M - 1)$ triplet pairs could be obtained. This exhaustive mini-batch strategy has become the standard operation for cross-view geo-localization methods trained with the triplet-based loss function.

CVM-Net: Hu et al. (2018) introduced NetVLAD (Arandjelović et al., 2018) into cross-view geo-localization. In detail, the authors combined a siamese network (Chopra et al., 2005) with NetVLAD (Arandjelović et al., 2018) to jointly learn discriminative features from the ground and aerial views. The authors proposed two models named CVM-Net-I and CVM-Net-II in which both share the same backbone architecture for extracting features.

CVM-Net-I optimized the parameters of the two NetVLAD layers (the satellite extractor and ground extractor) separately. However, the last convolutional layers and the NetVLAD layers of CVM-Net-II share the same parameters between the satellite extractor and ground extractor. To speed up the training and avoid manually choosing the margin, an improved weighted soft margin triplet loss was proposed. Because of the advanced architecture and the new loss function, CVM-Net achieved competitive results on the CVUSA Workman et al. (2015) and Vo (Vo & Hays, 2016) datasets. Figure 14 visualizes this approach.

FCBAM: Deep siamese-based methods usually depend on metric learning where performance is largely affected by the hard samples in the training data. It is well-proven that hard samples in the training data decrease the training quality at an early stage (Schroff, Kalenichenko, & Philbin, 2015). A similar pattern can also be observed in cross-view geo-localization methods which are trained with triplet loss. To alleviate this problem, (Cai, Guo, Khan, Hu, & Wen, 2019) proposed a Hard Exemplar Reweighting (HER) triplet loss. The HER triplet loss is adopted from the soft margin triplet loss in (Vo & Hays, 2016). The major difference is that the authors assign different weights for different triplets by a distance rectified logistic regression module. Another innovation in this paper is the Feature Context-Based Attention Module (FCBAM). FCBAM is inspired by the Convolutional Block Attention Module (CBAM) (Woo, Park, Lee, & Kweon, 2018) and Contextual Reweighting Network (CRN) (H.J. Kim et al., 2017). FCBAM is composed of a channel attention module that highlights the informative features for each channel, and a spatial attention module which captures the resulting features. The overview of the proposed model is shown in Figure 15.

OriCNN: Orientation information has been found to be helpful for cross-view image geo-localization (Vo & Hays, 2016). However, merging the orientation information with the CNN model is a challenging problem. Liu and Li (2019) proposed an efficient method to fuse the heading direction of ground-level images into a network and learn more robust features. The authors borrowed ideas from the color-coded map and designed a similar mechanism to encode the pixel-wise orientation information. The author proposed to encode the azimuth of two views into the U

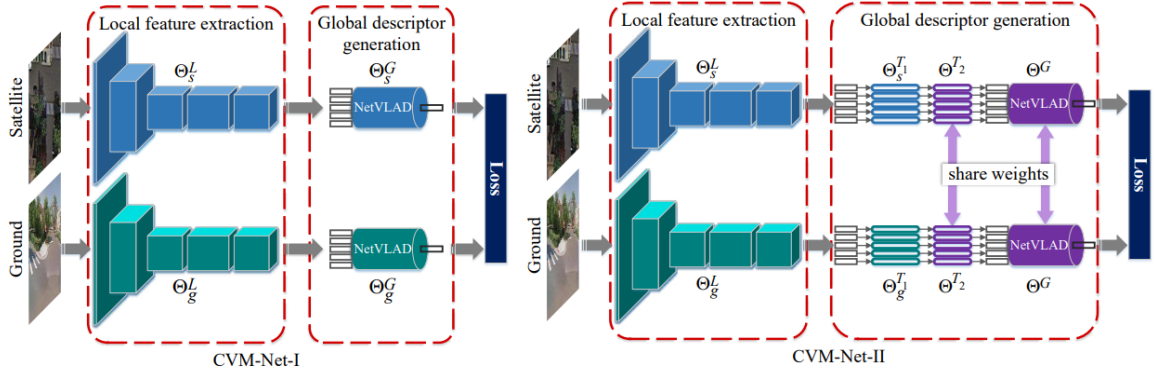


Fig. 14: The proposed two CVM architecture in (Hu et al., 2018). *CVM-Net-I* and *CVM-Net-II* share the same backbone feature extractor (Θ_s^L and Θ_g^L) The critical difference between the two networks is the architecture and the weight sharing between the global descriptor generation module. Figure is taken from (Hu et al., 2018)

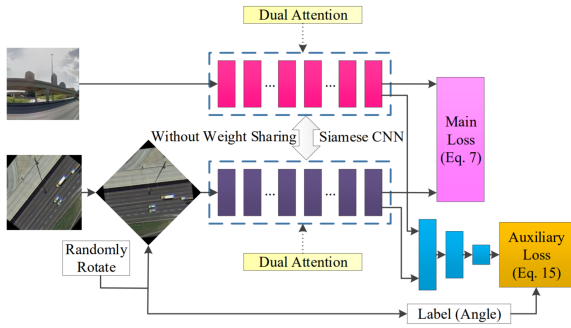


Fig. 15: The model proposed by (Cai et al., 2019). The model was composed of two dual attention networks for extracting features from aerial and ground perspectives respectively. An auxiliary subnetwork is adopted to predict the orientation of the randomly rotated input aerial image. Figure is taken from (Cai et al., 2019).

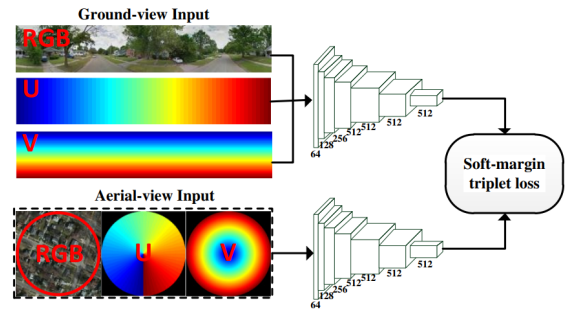


Fig. 16: Architecture of the OriCNN network proposed in (Liu & Li, 2019). The U channel represents the ‘azimuth’ for both views. The V channel contains the ‘altitude’ for ground view images and the ‘range’ for aerial view images. This figure is taken from (Liu & Li, 2019).

channel. The altitude of the ground view and the range of the aerial view is encoded in the V channel. A visualization is shown in Figure 16. The siamese network takes a stack containing the U channel and V channel as input. A weighted soft-margin triplet loss (Hu et al., 2018) is adopted for training the model. To better evaluate the performance, the authors also proposed a large-scale dataset, CVACT, containing $10x$ more samples than CVUSA in the testing set.

CVFT: Inspired by Optimal Transport (OT) theory, Shi, Yu, Liu, Zhang, and Li (2020) proposed a Cross-View Feature Transport (CVFT) layer for domain feature transferring which facilitates cross-view feature

matching. CVFT explicitly models the domain gap between aerial-view imagery and ground-view images by a transport matrix. Traditionally, OT is a linear programming problem that is computationally inefficient. To solve this problem, a different version (Cuturi, 2013) of OT, called a Sinkhorn solver (Knight, 2008; Sinkhorn & Knopp, 1967), which is based on entropy regularization was adopted. Finally, the feature transport problem was converted into a convex problem to be solved by a Sinkhorn solver. A diagram of their approach is provided in Figure 17.

SAFA: The main challenge of cross-view geolocalization is the domain gap between the aerial and ground views. By leveraging the prior geometric

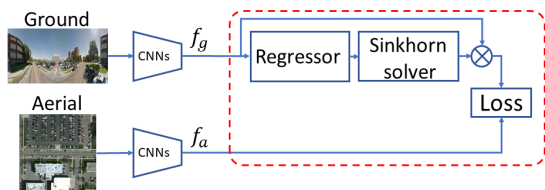


Fig. 17: The proposed pipeline of CVFT (Shi, Yu, Liu, et al., 2020). For ground input images, the features extracted by the backbone network are projected to the aerial feature domain using a learned feature transportation module (denoted as a dashed red box) which is composed of a regressor and a Sinkhorn solver. A soft-margin triplet loss is adopted to train the model.

knowledge between the two domains, Shi, Liu, Yu, and Li (2019) proposed a pre-processing technique that adopts a polar transformation on the aerial-view image. This technique bridges the visual domain gap between the ground-view images and the aerial images. The authors also proposed a spatial-aware feature aggregation network (SAFA) to capture global features from both aerial and ground images. Inspired by (Lazebnik, Schmid, & Ponce, 2006), the authors stacked multiple SAFAs in parallel to simultaneously aggregate features from different aspects. The proposed SAFA module and polar transformation largely improved the performance on the CVUSA (Workman et al., 2015) and CVACT (Liu & Li, 2019) datasets. However, the polar transformation proposed in this paper assumes the locations of the ground view images always align at the center of the aerial image, which is not always the case in real-world scenarios.

DSM: Most cross-view geolocation methods (Hu et al., 2018; Liu & Li, 2019; Workman et al., 2015) assume that the query images are panoramic ground-level images. (Shi, Yu, Campbell, & Li, 2020) focused on cross-view geo-localization on images with their heading orientation but a limited field of view. The authors proposed a Dynamic Similarity Matching (DSM) module to both measure the feature similarity between two views and their orientation using a sliding window. The proposed model is presented in Figure 18. Specifically, DSM takes the ground feature and the aerial feature extractors as input. Then a shifting window slides across the ground features to compute the inner product with the aerial features. The location of the highest inner product value indicated the orientation and similarity. Note that the

polar transformation is one of the pre-processing steps in this paper.

VIGOR: Previous existing datasets assume that there is a one-to-one correspondence between ground-view images and aerial-view images. To address this limitation, S. Zhu et al. (2021b) proposed a new dataset that has a many-to-one correspondence between the ground and aerial images. This dataset is densely sampled in four USA cities and grabbed panoramic images from Google Street View (GSV) (Anguelov et al., 2010). The authors proposed three categories to define cross-view matching: positive, semi-positive, and negative. Positive and negative pairs are the same as in CVUSA and CVACT. In the semi-positive pairs, the ground-view location appears in aerial-view images but not in the center region. By doing so, cross-view geo-localization becomes a many-to-one retrieval problem rather than a one-to-one retrieval problem. This configuration is more realistic and closer to real-life deployment. Besides the many-to-one retrieval formation, VIGOR also achieved meter-level offset prediction of the camera location by utilizing an offset prediction subnetwork. Their experiments demonstrated that the noisy GPS coordinates can be refined using the offset prediction subnetwork. The proposed model in this paper adopted the same architecture as SAFA (Shi et al., 2019) with the proposed offset prediction subnetwork as shown in Figure 19. The authors also proposed an IOU-based loss function to guide the network in learning features from semi-positive samples.

AlignNet: S. Zhu, Yang, and Chen (2021a) studied the effect of orientation alignment between ground images and aerial images. The authors found that some existing algorithms are unfair due to aligning the orientation between two views in both training and testing as prior. The authors proposed a novel method for alignment angle regression using the output from Grad-CAM (Selvaraju et al., 2017). Moreover, a new loss function that can balance the gradient of positive pairs and negative pairs was proposed. Finally, the authors proposed a new global mining strategy for training the model with hard samples from full datasets rather than inside a mini-batch as was typical in previous works.

Seeing the Unseen: Rodrigues and Tani (2021) proposed a novel data augmentation pipeline for cross-view geo-localization. The authors utilized the

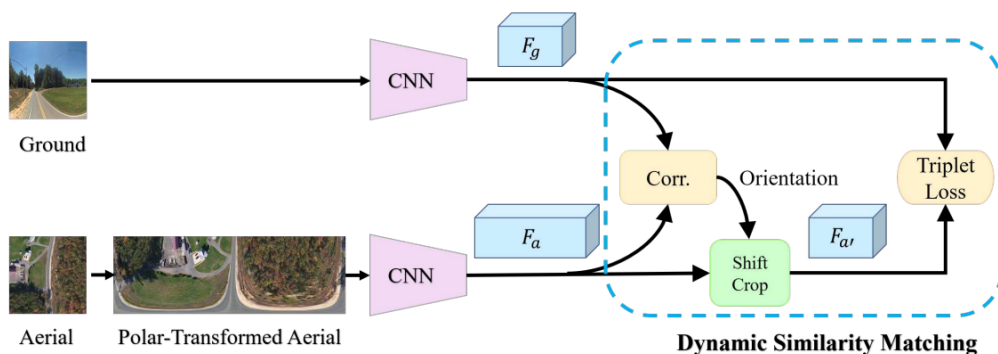


Fig. 18: The proposed architecture for the Dynamic Similarity Matching (DSM) (Shi, Yu, Campbell, & Li, 2020) network. The DSM module estimates the orientation of the ground image by sliding and matching between the feature maps of ground images and polar transformed aerial images. Figure is taken from (Shi, Yu, Campbell, & Li, 2020)

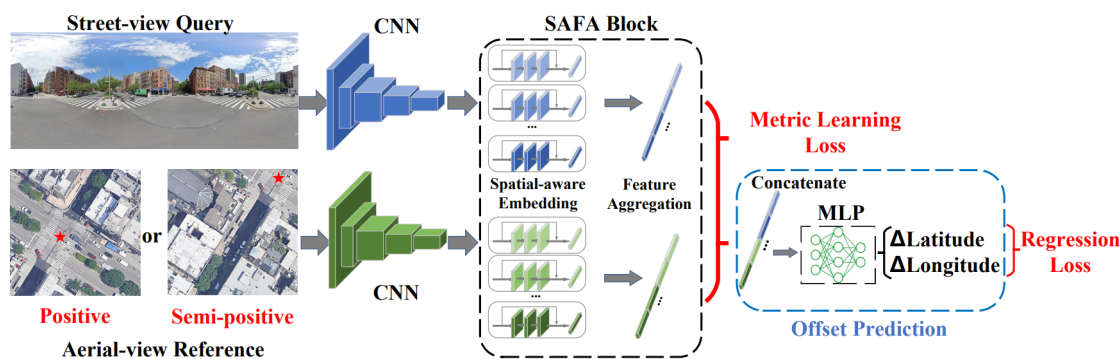


Fig. 19: Architecture of the method proposed by (S. Zhu et al., 2021b). The SAFA blocks aggregate the raw features extracted by backbone CNNs. A subnetwork predicts the offset latitude and longitude to determine the exact location of the ground image by taking the predicted features as input. This architecture is the same as (Shi et al., 2019) except for the additional offset prediction branch.

segmentation map from existing models to cut out the objects (buildings, sidewalks, sky, etc.) in the **ground-view** images to force the network to learn from the unseen objects and perform unseen object matching. Apart from the novel data augmentation pipeline, a multi-scale attention module was proposed for the matching task.

LPN: T. Wang et al. (2021) proposed a Local Pattern Network (LPN) which is an end-to-end learnable model able to extract features globally from both **aerial and ground-view** images. Fig 20 shows the structure of the LPN. The key idea of the LPN is to force the network to focus on the contextual information in the neighboring areas using the square-ring partitioning strategy shown in the green box of Fig 20.

To be noticed, unlike any methods introduced in this section, LPN uses a multi-class cross-entropy loss for training. During the testing, features before the classification layer are used for estimating the similarity by cosine distance. This approach is visualized in Figure 20.

TransGeo: Transformers and multi-head attention mechanisms (Vaswani et al., 2017) have been developing rapidly in recent years. The capability of the transformer to explore the global correlations significantly boosts the performance of cross-view geo-localization research. S. Zhu, Shah, and Chen (2022) is one of the pioneers to apply transformers to this field. Their proposed TransGeo model is presented in Figure 21. TransGeo is composed of two

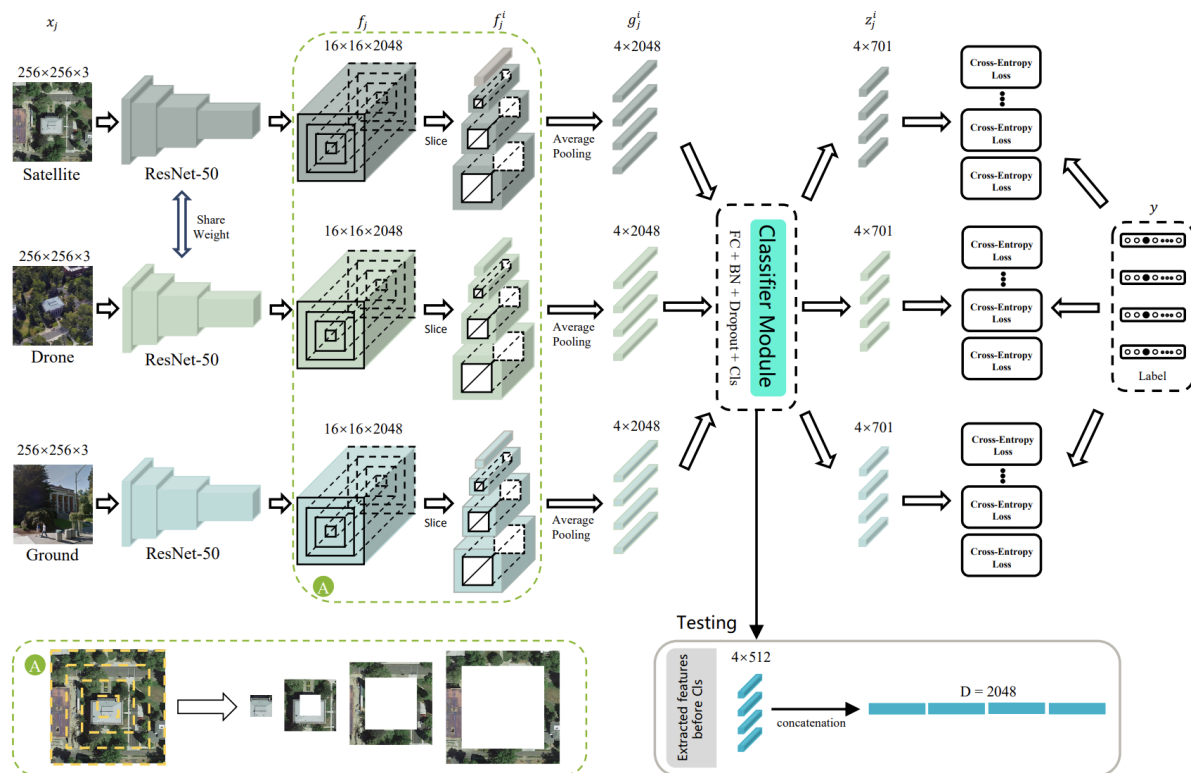


Fig. 20: An overview of the Local Pattern Network (LPN) proposed by (T. Wang et al., 2021). The proposed square-ring partitioning strategy generates latent features from the input images at different scales of neighboring areas. The LPN network utilizes a classification module to learn a latent space representation. Figure is taken from (T. Wang et al., 2021)

main parts, namely a street-view transformer encoder and an aerial-view transformer encoder. Both transformer encoders are employed from the pre-trained DeiT (Touvron et al., 2021) model. A special two-stage training paradigm is proposed to train TransGeo. In the first stage, the model is trained by the normal soft-margin triplet loss. In the second stage, based on the saliency attention map from the aerial-view transformer encoder, non-uniform cropping is applied to the aerial image to extract more fine-grained features. Benefiting from the advanced transformer architecture and two-stage training paradigm, TransGeo (S. Zhu et al., 2022) is considered one of the best models in cross-view geo-localization and achieves superior performance on popular benchmarks.

GeoDTR: Most cross-view geo-localization methods aim to implicitly learn the geometric layout similarity by matching the learned latent features. GeoDTR (X. Zhang, Li, Sultani, Zhou, & Wshah,

2023) addresses this issue by explicitly capturing the geometric layout information from both aerial and ground images via a trainable geometric layout extractor which consists of 2 transformers, as presented in Figure 22. To tackle the issue of lacking ground truths for the geometric layouts, a counterfactual learning scheme is proposed to provide weak supervision signals to train the model. To further alleviate the issue of overfitting to low-level details, the authors proposed layout simulation and semantic augmentation (LS) to augment training data. Unlike existing data augmentation methods, the authors argue LS does not break the correspondences between aerial and ground image pairs. LS maintains the correspondences while diversifying the geometric layout and low-level details of the training data.

4.4 Generative Methods

Since the proposal of Generative Adversarial Networks (GAN) (Goodfellow et al., 2014) in 2014,

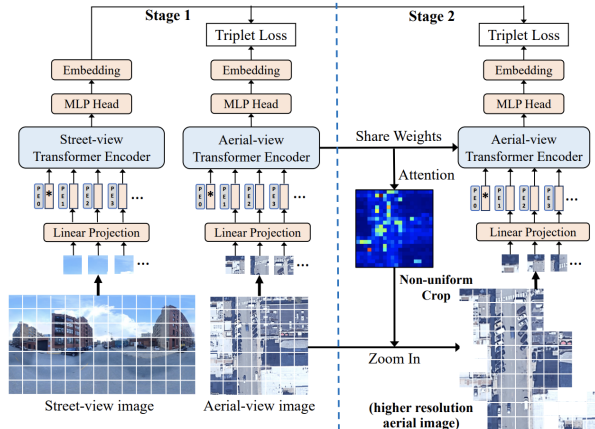


Fig. 21: An overview of the TransGeo (S. Zhu et al., 2022) model. The model contains a street-view transformer encoder and an aerial-view transformer encoder. In the first stage, the model is trained by a soft-margin triplet loss. In the second stage, the model crops the important regions from the aerial view for fine-grained feature extraction. Figure is taken from (S. Zhu et al., 2022).

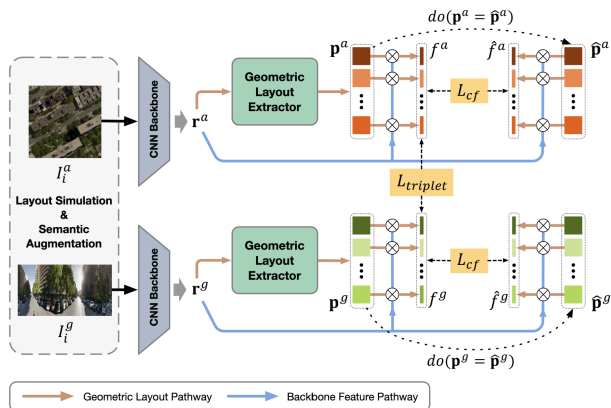


Fig. 22: An overview of the GeoDTR (X. Zhang, Li, et al., 2023) model. Each aerial and ground image pair is first augmented by the proposed layout simulation and semantic augmentation. The geometric layout extractor then extracts layout information from the raw features. The do operation stands for the counterfactual learning schema. The predicted features are the Frobenius product between the layout features and the raw features. Figure is taken from (X. Zhang, Li, et al., 2023).

image **synthesis** has increasingly been dominated by GANs. Due to **their** ability to generate realistic images, GANs have been applied in diverse applications such as image synthesis (Brock, Donahue, & Simonyan, 2019; Goodfellow et al., 2014; Karras, Laine, & Aila, 2019), image-to-image translation (Isola, Zhu, Zhou, & Efros, 2017; Pumarola, Agudo, Martinez, Sanfeliu, & Moreno-Noguer, 2018; Tang, Liu, Xu, Torr, & Sebe, 2021; Yi, Zhang, Tan, & Gong, 2017; J.-Y. Zhu, Park, Isola, & Efros, 2017; J.-Y. Zhu, Zhang, et al., 2017), and super resolution (Ledig et al., 2017; X. Wang et al., 2018). To this end, researchers also explored the relationship between satellite and ground images. For example, given an **aerial-view** image, a model learns to generate a **ground-view** image that keeps the visual features from the aerial image (building, road, tree, etc). Zhai et al. (2017) first discovered that **ground-view** scene layouts can be generated from a segmentation map of an aerial image. Regmi and Borji (2018) proposed two models named as X-Fork and X-Seq. These models generate street-view images and corresponding segmentation maps using only **aerial-view** images as input by leveraging a conditional GAN (Mirza & Osindero, 2014). Tang et al. (2019) proposed SelectionGAN which utilized a multi-channel selection module to obtain better quality for the final generated **ground-view** images. More recently, predicting satellite depths and further taking advantage of geometric transformations to estimate **ground-view** panoramic images is becoming a new trend. Shi, Campbell, Yu, and Li (2021) proposed a satellite-to-street-view image projection (S2SP) module to achieve this goal. Whereas, Lu et al. (2020) achieved this by employing a panoramic projection via generating an occupancy grid from depth maps and the first encountering voxels in the generated occupancy grid. After geometric transformation, the result is fed into a generator which produces the final street-view image. For example, BiCycleGAN (J.-Y. Zhu, Zhang, et al., 2017) is employed after the panoramic projection in (Lu et al., 2020). Although the methods mentioned above are not cross-view geo-localization methods, they have inspired the following cross-view geo-localization methods which use GANs to boost the performance of cross-view geo-localization methods.

SAFA-GAN: Siamese-like CNN models easily neglect low-level detail because the triplet loss and its variants do not have constraints on them. However,

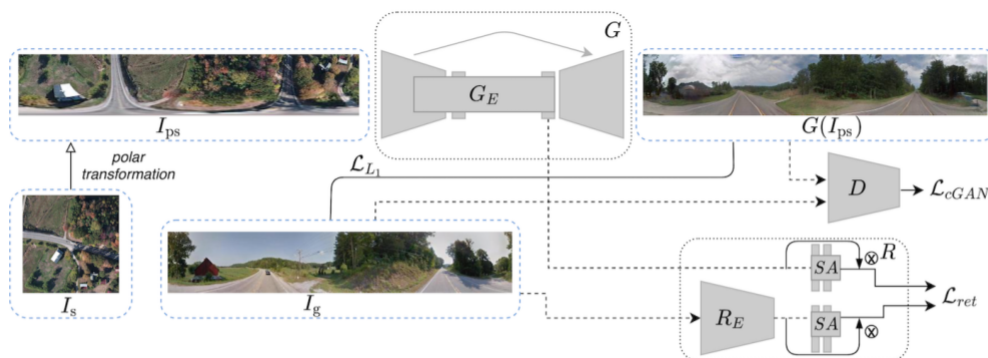


Fig. 23: An overview of SAFA-GAN proposed by (Toker et al., 2021). A GAN G and D is adopted to perform ground image synthesis by taking the polar transformed aerial image as input. Then, a SAFA module (SA) is employed to train the model which performs cross-view geo-localization. R_E is a learnable submodule to map the ground image to the learned latent feature space. This figure is taken from (Toker et al., 2021).

low-level details are useful when incorporated into the cross-view geo-localization task. To accomplish this, Toker et al. (2021) proposed to learn discriminative features between satellite and street images using a Generative Adversarial Network (Goodfellow et al., 2014). The proposed network is composed of a GAN (Goodfellow et al., 2014) that maps a polar transformed aerial-view image to a synthetic street-view image, and a SAFA-based (Shi et al., 2019) subnetwork to perform cross-view geolocation task. The proposed model is shown in Figure 23. The intermediate features from the generator are then reused in the retrieval subnetwork for cross-view geolocation. In this manner, the two tasks, retrieval and generation, mutually learn from each other to create a feature representation informative for both tasks.

Feature Fusion GAN: Regmi and Shah (2019) proposed a novel feature fusion training strategy in which the features from synthesized satellite imagery are fused with corresponding street-view features. An overview of the proposed method is shown in Figure 24. To synthesize a satellite view from a street view, the authors adopted the generator from X-Fork (Regmi & Borji, 2018). Two CNNs (Krizhevsky et al., 2012) are used to extract satellite features and street view features independently. After fusing the street view features and the generated satellite view features with a fully connected network, feature matching is performed between the output of the fully connected network and the ground truth satellite. This model pushed the performance of

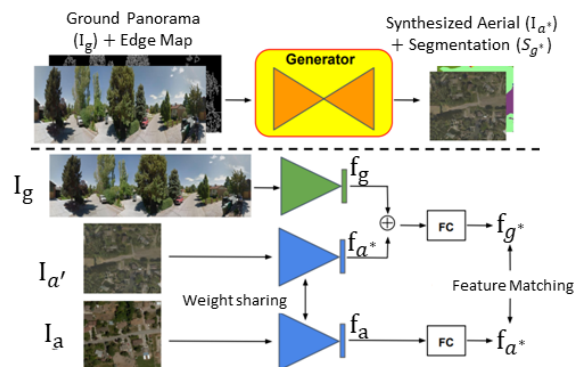


Fig. 24: The method proposed in (Regmi & Shah, 2019). The upper panel is the X-Fork (Regmi & Borji, 2018) generator which generates satellite images from ground images. The bottom panel illustrates the proposed feature fusion schema. The blue module extracts features from real satellite images I_a and generated satellite images $I_{a'}$. The ground features I_g are extracted from the green layer module. I_g and $I_{a'}$ are fused by a fully connected layer. The fusion algorithm aims to push the fused features f_{g^*} and aerial features f_{a^*} closer in the latent space. The figure is taken from (Regmi & Shah, 2019).

cross-view geo-localization by a large margin on the CVUSA (Workman et al., 2015) dataset.

Method	Type	Deep Learning vs. Traditional	Polar Transformation	Year
AVG & DT (Lin et al., 2013)	Hand-Crafted Feature	Traditional	No	2013
Semantic cross-view matching (Castaldo et al., 2015)	Hand-Crafted Feature	Traditional	No	2015
Building matching (Tian et al., 2017)	Graph-Based	Deep Learning+ Dominant Set	No	2017
Landmark matching (Verde et al., 2020)	Graph-Based	Traditional	No	2020
Where-CNN (Lin et al., 2015)	Siamese-Like Network	Deep Learning	No	2015
MCVPlaces (Workman et al., 2015)	Siamese-Like Network	Deep Learning	No	2015
DBL (Vo & Hays, 2016)	Siamese-Like Network	Deep Learning	No	2016
CVM-Net (Hu et al., 2018)	Siamese-Like Network	Deep Learning	No	2018
FCBAM (Cai et al., 2019)	Siamese-Like Network	Deep Learning	No	2019
OriCNN (Liu & Li, 2019)	Siamese-Like Network	Deep Learning	No	2019
Feature Fusion GAN (Regmi & Shah, 2019)	Generative	Deep Learning	No	2019
CVFT (Shi, Yu, Liu, et al., 2020)	Siamese-Like Network	Deep Learning	No	2020
SAFA (Shi et al., 2019)	Siamese-Like Network	Deep Learning	Yes	2020
DSM (Shi, Yu, Campbell, & Li, 2020)	Siamese-Like Network	Deep Learning	Yes	2020
VIGOR (S. Zhu et al., 2021b)	Siamese-Like Network	Deep Learning	No	2021
AlignNet (S. Zhu et al., 2021a)	Siamese-Like Network	Deep Learning	No	2021
Seeing the Unseen (Rodrigues & Tani, 2021)	Siamese-Like Network	Deep Learning	No	2021
LPN (T. Wang et al., 2021)	Siamese-Like Network	Deep Learning	No	2021
SAFA-GAN (Toker et al., 2021)	Generative	Deep Learning	Yes	2021
TransGeo (S. Zhu et al., 2022)	Siamese-Like Network	Deep Learning	No	2022
GeoDTR (X. Zhang, Li, et al., 2023)	Siamese-Like Network	Deep Learning	Yes	2023

Table 6: Summary of cross-view geo-localization methods.

4.5 Summary of cross-view geo-localization methods

Cross-view geo-localization is a difficult task due to the extreme differences in views, varying photo-taking time, and inconsistent resolution between two views. Before the deep learning era, most works struggled with the accuracy of models. With the advancement of deep learning, the performance of cross-view geo-localization methods has increased drastically. However, deep learning models are analogous to a black box. The lack of explainability hinders the development of deep-learning-based cross-view geo-localization methods. Graph-based methods maintain better explainability but are either not scalable to large-scale datasets (Verde et al., 2020) or only work on areas with highly distinguishable objects (i.e. skyscrapers) (Tian et al., 2017). Despite lacking explainability, several polar-transformation-based methods (Shi et al., 2019; Shi, Yu, Campbell, & Li, 2020; Toker et al., 2021; X. Zhang, Li, et al., 2023) have achieved state-of-the-art performance. Polar transformations, as a pre-processing technique, assume the camera location lies at the center of an **aerial-view** image. This strong requirement can rarely be achieved during deployment in real-world scenarios. More recent works such as VIGOR (S. Zhu et al., 2021b) address this problem by proposing to estimate the shift in the camera’s location. However, the performance still has significant room for improvement. A brief summary of all the introduced cross-view geo-localization methods is presented in Table 6.

With the rapid development of cross-view image geo-localization, it is a natural idea to extend cross-view image geo-localization to cross-view video geo-localization. To tackle this problem, some existing methods studied different categories of temporal information aggregation methods. For example, Seq-Geo (X. Zhang, Sultani, & Wshah, 2023) and CVL-Net (Shi, Yu, Wang, & Li, 2022) proposed to use transformers to aggregate the temporal features from ground images. On the hand, **GAMA** (Vyas, Chen, & Shah, 2022) utilized a 3D CNN to gather the ground sequential information but adopted a transformer to extract spatial information from an aerial view. Cross-view video geo-localization is still a new research area and is out of scope in this section. Thus, we will not benchmark the above-mentioned cross-view video geo-localization methods in the following sections.

4.6 Cross-View Image Geo-localization Datasets

CVUSA:¹² CVUSA (Workman et al., 2015) is the first large-scale cross-view geo-localization dataset containing street-view images downloaded from GSV (Anguelov et al., 2010) and Flickr¹³. The satellite images were obtained from Bing Maps¹⁴. Specifically, GSV images were gathered from random locations in the USA, and the Flickr images were

¹²<http://mvr1.cs.uky.edu/datasets/cvusa/>

¹³<https://www.flickr.com/>

¹⁴<https://www.bing.com/maps/>



Fig. 25: The top two rows display sample images from the CVUSA (Workman et al., 2015) dataset and the bottom two rows display sample images from the CVACT (Liu & Li, 2019) dataset. On the left is a satellite image and on the right side is its corresponding ground-level panorama.

sampled and downloaded from the grid of 100×100 locations on a map of the USA. Finally, given the location of each ground image, corresponding satellite images with a resolution of 800×800 were downloaded from Bing Maps. In total, this dataset contains 879,318 unique locations and a total of 1,588,655 ground-satellite pairs. The well-known CVUSA benchmark is a refinement of the version from (Zhai et al., 2017). It includes 35,532 ground-satellite pairs for training and 8,884 ground-satellite pairs for evaluation. Two sample images from the refined version are presented on the top two rows of Figure 25. In the rest of this paper, we refer ‘CVUSA’ as the refined version unless otherwise specified.

CVACT:¹⁵ CVACT (Liu & Li, 2019) covers 300 square miles of road in Canberra, Australia. To collect street and satellite images, the GSV API¹⁶ and Google Maps API was employed. All street view images (panoramas) were captured at zoom level 2 at a resolution of 1664×832 and satellite images were captured at zoom level 20 at a resolution of 1200×1200 . Two sample images in this dataset are presented in the bottom two rows of Figure 25. In

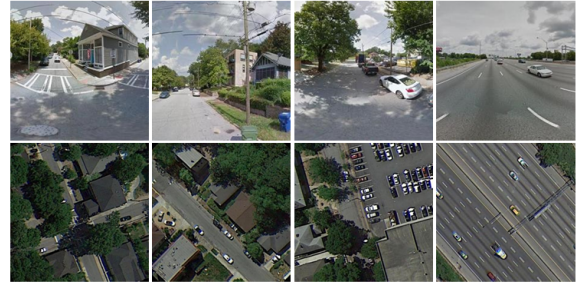


Fig. 26: Four sample images from Vo (Vo & Hays, 2016) dataset. The top row shows the ground images and the bottom row shows the corresponding aerial images.

total, this dataset contains 128,334 ground-satellite image pairs of which 35,532 pairs are used for training, 8,884 for validation, denoted as CVACT_val, and 92,802 for testing, denoted as CVACT_test.

Vo:¹⁷ Vo (Vo & Hays, 2016) is a large-scale dataset containing more than 1 million ground-aerial image pairs. Four sample images are shown in Figure 26. Different from other datasets mentioned in this section, this dataset focuses on localizing the scenes in the image (assuming the main object lies at the center of the satellite image) rather than the location of the camera. For example, in the first column of Figure 26, the center area of the satellite image is the building which is the main object in the ground image. This is in contrast to the CVUSA (Workman et al., 2015) and CVACT (Liu & Li, 2019) datasets. To achieve this goal, the authors queried street-view panoramic images from GSV (Anguelov et al., 2010) and split them into several crops. For each crop, they obtained the depth estimation from GSV and downloaded the corresponding satellite image using the Google Maps API¹⁸. The ground panoramas were randomly collected from 11 different US cities by employing GSV (Anguelov et al., 2010).

UrbanGeo:¹⁹ Tian et al. (2017) focused on cross-view geo-localization in urban areas and collected data from three cities in the U.S. including Pittsburgh,

¹⁷<https://github.com/lugiavn/gt-crossview>

¹⁸<https://developers.google.com/maps/documentation/maps-static/overview>

¹⁹<https://www.crcv.ucf.edu/research/cross-view-image-matching-for-geo-localization-in-urban-environments/>

¹⁵<https://github.com/Liumouliu/OriCNN>

¹⁶<https://developers.google.com/maps/documentation/streetview/overview>

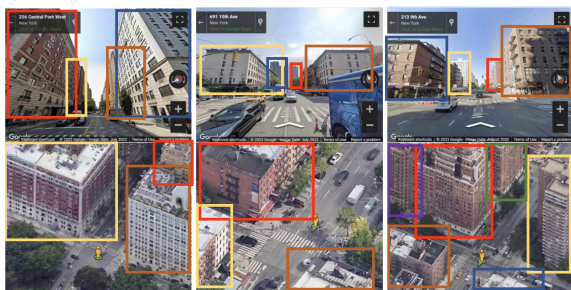


Fig. 27: 3 Demonstration images pairs from Urban-Geo (Tian et al., 2017) dataset. The top rows are ground-level images and the bottom rows are corresponding bird's eye view images. The bounding boxes are detected buildings. The image is taken from (Tian et al., 2017).



Fig. 28: Sample images from VIGOR (S. Zhu et al., 2021b) dataset. On the left are two ground-level images covered by the satellite image on right. The yellow line in the ground-level images represents north direction. The color of the star in the satellite image represents the location of the ground-level image with same color border. This image is taken from (S. Zhu et al., 2021b).

Orlando and part of Manhattan. The author collected 8,851 GPS points in total from these three cities. For each GPS location, 4 different bird's eye view images were captured with heading orientations of 0° , 90° , 180° , 270° , respectively. DualMaps²⁰ was employed to obtain corresponding street view images from GSV (Anguelov et al., 2010) by a given bird's eye view image. Furthermore, the author annotated each building's bounding boxes on street view images as well as on bird's eye view images if it co-exists in both views. Sample images are shown in Figure 27.

VIGOR:²¹ S. Zhu et al. (2021b) collected VIGOR dataset which contains densely sampled locations from four US cities namely: New York City (Manhattan), San Francisco, Chicago, and Seattle, using the Google Maps API and GSV API. As compared to the previously mentioned dataset (Liu & Li, 2019; Vo & Hays, 2016; Workman et al., 2015), VIGOR is more challenging due to the presence of occlusion and shadows by tall buildings in metropolitan areas. Furthermore, this dataset is obtained in more realistic settings. First, the query images and the ground truth reference images do not exactly align with the center like previous datasets (Liu & Li, 2019; Workman et al., 2015). Second, the location of a query ground-level image may be covered by several reference satellite images. VIGOR contains 90,618 aerial images and 105,214 ground panoramas. Satellite images were captured at a zoom level²² of 20 (equivalent to a ground resolution of $0.149m$) with an image resolution of 640×640 . The ground images were obtained with a resolution of 2048×1024 . A sample image is shown in Figure 28. VIGOR designed two evaluation settings, called same-area protocol and cross-area protocol. Same-area protocol includes data from all 4 cities for training and evaluation. On the other hand, cross-area protocol includes images from New York and Seattle for training, and images from San Francisco and Chicago for evaluation.

University-1652:²³ University-1652 (Z. Zheng et al., 2020) is a newly captured drone-based geo-localization dataset. Unlike the aerial-ground datasets (Liu & Li, 2019; Vo & Hays, 2016; Workman et al., 2015; S. Zhu et al., 2021b), University-1652 provides three modalities, drone-view, ground-view, and satellite-view. To capture drone views, the authors synthesized images from Google Earth²⁴. Two sample locations are shown in Figure 29. Different from the other datasets in this section which focus on generic cross-view geo-localization, University-1652 highlights the building matching between the three modalities. To this end, University-1652 was built with 1652 different buildings in which 1402 buildings contain all 3 modalities. The author split these 1402

²⁰<http://www.mapchannels.com/DualMaps.aspx>

²¹<https://github.com/Jeff-Zilence/VIGOR>

²²https://wiki.openstreetmap.org/wiki/Zoom_levels

²³<https://github.com/layumi/University1652-Baseline>

²⁴<https://earth.google.com/web/>



Fig. 29: Two sample locations from University-1652 (Z. Zheng et al., 2020) dataset. The first row is the ground-level view, the second row is the aerial view, and the bottom row is the drone view. This image is taken from (Z. Zheng et al., 2020).



Fig. 30: Sample images from DeepGeo (Lin et al., 2015) dataset. The top row shows five ground-level images. The bottom row shows their corresponding oblique views. This image is taken from (Lin et al., 2015).

buildings into training and test sets equally. On average, each building appears in 54 drone views, 3.38 ground views, and 1 satellite view. To be noticed, there is an extra ground view training dataset collected from search engines which results in 16.64 ground view images per building.

DeepGeo: Lin et al. (2015) proposed DeepGeo which contains 1.1M ground and oblique aerial images.

There are around 40K matched pairs and the remaining are unmatched images in the dataset. To capture the corresponding point of interest in oblique satellite imagery, they performed an automatic generation process which includes a coarse depth plan estimation (Anguelov et al., 2010) followed by an image re-projection. Sample images from this dataset are shown in Figure 30. This dataset is not publicly available.

4.7 Evaluation Metrics

The performance of cross-view image geo-localization approaches is usually evaluated by three measurements, recall accuracy at top- K ($R@K$), Average Precision (AP), and hit rate. $R@K$, which is similar to the ‘Reference Ranking’ evaluation metric for single-view geo-localization mentioned in Section 3, is the most popular evaluation metric in cross-view geo-localization and has been used in every dataset as mentioned in Section 4.6. K stands for the top K closest matching samples in reference images for a given query image. Euclidean distance is typically employed to measure the similarity (Hu et al., 2018; Liu & Li, 2019; Shi et al., 2019; Toker et al., 2021; S. Zhu et al., 2021b). For one-to-one retrieval tasks (Liu & Li, 2019; Vo & Hays, 2016; Workman et al., 2015), it is sufficient to evaluate using a top- K ranking. However, for many-to-one retrieval tasks (Z. Zheng et al., 2020; S. Zhu et al., 2021b), top- K ranking is not sufficient to evaluate the performance of the algorithms on multiple true-matched reference images. Thus, University-1652 (Z. Zheng et al., 2020) adopted the Average Precision (AP) metric which is the area under the precision-recall curve. In VIGOR (S. Zhu et al., 2021b), the authors proposed hit rate to evaluate the performance in the many-to-one retrieval task. If the retrieved top-1 image covers the query image, it is considered to be a hit. The hit rate is calculated as the ratio of queries correctly hit to the total number of query images. Table 7 summarizes the key aspects of all the introduced cross-view geo-localization datasets in section 4.6 as well as their evaluation metrics.

4.8 Benchmarks

In this section, we present experimental results on the cross-view geo-localization methods mentioned in previous sections.

Experiments on CVUSA (Workman et al., 2015):

	CVUSA (Workman et al., 2015)	CVACT (Liu & Li, 2019)	Vo (Vo & Hays, 2016)	UrbanGeo (Tian et al., 2017)	DeepGeo (Lin et al., 2015)	VIGOR (S. Zhu et al., 2021b)	University-1652 (Z. Zheng et al., 2020)
# of aerial images	44,416	128,334	≈1M	≈30K	≈80K	90,618	1652
# of ground images	44,416	128,334	≈1M	≈30K	≈80K	90,618	11,664
# of drone-view images	-	-	-	-	-	-	89,210
Coverage	Urban,Suburb	Urban,Suburb	Urban,Suburb	Urban	Urban	Urban	Building only
GPS information	Yes	Yes	Yes	Yes	Yes	Yes	Yes
Evaluation metrics	R@K	R@K	R@K	AP, PR curves	AP, PR curves	R@K, Hit Rate	R@K, AP

Table 7: Summary of cross-view geo-localization datasets. ‘R@K’ is short for recall at top K.

CVUSA (Workman et al., 2015)				
Method	R@1	R@5	R@10	R@1%
MCVPlaces (Workman et al., 2015)	-	-	-	34.30
DBL (Vo & Hays, 2016)	-	-	-	63.70
CVM-Net-I (Hu et al., 2018)	22.47	49.98	63.18	93.62
OriCNN (Liu & Li, 2019)	31.71	56.61	67.57	93.19
FCBAM (Cai et al., 2019)	-	-	-	98.30
Feature Fusion GAN (Regmi & Shah, 2019)	48.75	-	81.27	95.98
CVFT (Shi, Yu, Liu, et al., 2020)	61.43	84.69	90.49	99.02
AlignNet (S. Zhu et al., 2021a)	54.50	-	-	97.70
Seeing the Unseen (Rodrigues & Tani, 2021)	75.95	91.90	95.00	99.42
SAFA (Shi et al., 2019)	89.84	96.93	98.14	99.64
LPN (T. Wang et al., 2021)	85.79	95.38	96.98	99.41
DSM (Shi, Yu, Campbell, & Li, 2020)	91.96	97.50	98.54	99.67
SAFA-GAN (Toker et al., 2021)	92.56	97.55	98.33	99.57
TransGeo (S. Zhu et al., 2022)	94.08	98.36	99.04	99.77
GeoDTR (X. Zhang, Li, et al., 2023)	95.43	98.86	99.34	99.86

Table 8: Benchmark comparison on CVUSA (Workman et al., 2015) dataset.

CVACT_val (Liu & Li, 2019)				
Method	R@1	R@5	R@10	R@1%
CVM-Net-I (Hu et al., 2018)	20.15	45.00	56.87	87.57
OriCNN (Liu & Li, 2019)	46.96	68.28	75.48	92.01
CVFT (Shi, Yu, Liu, et al., 2020)	61.05	81.33	86.52	95.93
SAFA (Shi et al., 2019)	81.03	92.8	94.84	98.1
LPN (T. Wang et al., 2021)	79.99	90.63	92.56	97.03
Seeing the Unseen (Rodrigues & Tani, 2021)	73.19	90.39	93.38	97.45
DSM (Shi, Yu, Campbell, & Li, 2020)	82.49	92.44	93.99	97.32
SAFA-GAN (Toker et al., 2021)	83.28	93.57	95.42	98.22
TransGeo (S. Zhu et al., 2022)	84.95	94.14	95.78	98.37
GeoDTR (X. Zhang, Li, et al., 2023)	86.21	95.44	96.72	98.77

Table 9: Benchmark comparison on CVACT (Liu & Li, 2019) validation set.

As compared to other datasets, most of the methods are benchmarked on the **CVUSA dataset** (Workman et al., 2015), due to being the first large-scale cross-view geo-localization dataset. The experimental results are presented in Table 8. As expected MCVPlaces (Workman et al., 2015) performed the worst in the benchmark because it is the first proposed method. CVM-Net (Hu et al., 2018) improved the accuracy by a large margin. The recall accuracy at top-1 was improved to around 22% and the recall accuracy at top-1% was improved to above 90%. The second large

CVACT_test (Liu & Li, 2019)				
Method	R@1	R@5	R@10	R@1%
CVM-Net-I (Hu et al., 2018)	4.06	16.89	24.66	56.38
OriCNN (Liu & Li, 2019)	19.9	34.82	41.23	63.79
CVFT (Shi, Yu, Liu, et al., 2020)	34.39	58.83	66.78	95.99
SAFA (Shi et al., 2019)	55.5	79.94	85.08	94.49
DSM (Shi, Yu, Campbell, & Li, 2020)	35.55	60.17	67.95	86.71
SAFA-GAN (Toker et al., 2021)	61.29	85.13	89.14	98.32
GeoDTR (X. Zhang, Li, et al., 2023)	64.52	88.59	91.96	98.74

Table 10: Benchmark comparison on CVACT (Liu & Li, 2019) testing set.

Vo (Vo & Hays, 2016)	
Method	R@1%
MCV (Workman et al., 2015)	15.40
DBL (Vo & Hays, 2016)	15.90
CVM-I (Hu et al., 2018)	59.90
CVM-II (Hu et al., 2018)	67.90
AlignNet (S. Zhu et al., 2021a)	88.30

Table 11: Benchmark comparison on Vo (Vo & Hays, 2016) testing set. MCV stands for MCVPlaces (Workman et al., 2015). CVM-I and CVM-II stand for CVM-Net-I (Hu et al., 2018) and CVM-Net-II (Hu et al., 2018) respectively.

improvement was brought by SAFA (Shi et al., 2019) because of its feature aggregation techniques and the polar transformation. The recall accuracy at top-1 was improved to nearly 90%.

Experiments on CVACT (Liu & Li, 2019): The validation set of CVACT (Liu & Li, 2019) includes the same number of ground-satellite pairs as that of the CVUSA (Workman et al., 2015) testing set. However, the testing set for CVACT (Liu & Li, 2019) dataset has 10 times more ground-satellite pairs than the CVUSA (Workman et al., 2015) testing set. Thus we report the results on both of them. The results of the CVACT validation set (CVACT_val) are reported in Table 9. We observe that every method has a performance drop on the CVACT validation set as compared to their performance on the CVUSA (Workman et al., 2015) dataset. One reason is that CVACT (Liu & Li,

VIGOR (S. Zhu et al., 2021b)

Method	Same-Area				Cross-Area			
	R@1	R@5	R@1%	Hit Rate	R@1	R@5	R@1%	Hit Rate
SAFA (Shi et al., 2019)	33.9	58.4	98.2	36.9	8.2	19.6	77.6	8.9
SAFA (Shi et al., 2019) + Mining (S. Zhu et al., 2021a)	38.0	62.9	97.6	41.8	9.2	21.1	77.8	9.9
VIGOR (S. Zhu et al., 2021b)	41.1	65.8	98.4	44.7	11.0	23.6	80.2	11.6
TransGeo (S. Zhu et al., 2022)	61.48	87.54	99.56	73.09	18.99	38.24	88.94	21.21

Table 12: Benchmark comparison on VIGOR (S. Zhu et al., 2021b) testing set.

University-1652 (Z. Zheng et al., 2020)

Method	R@1	AP
CVM-Net-I (Hu et al., 2018)	53.21	58.03
Where-CNN (Lin et al., 2015)	52.39	57.44
Baseline (Z. Zheng et al., 2020)	58.49	63.31
LPN (T. Wang et al., 2021)	75.93	79.14

Table 13: Benchmark comparison on University-1652 (Z. Zheng et al., 2020) testing set.

2019) is densely captured in one single city. Therefore, the ground images in CVACT have less visual distinction than ground images in CVUSA (Workman et al., 2015) dataset. However, SAFA (Shi et al., 2019), DSM (Shi, Yu, Campbell, & Li, 2020), SAFA-GAN (Toker et al., 2021), TransGeo (S. Zhu et al., 2022), and GeoDTR (X. Zhang, Li, et al., 2023) still achieved greater than 80% accuracy on $R@1$ on CVACT validation (CVACT_val) benchmark. The CVACT testing set (CVACT_test) is even more challenging than the validation set due to its large-scale ground and aerial images. In Table 10, we observe that the performance of all methods drops further, where only GeoDTR (X. Zhang, Li, et al., 2023) achieved 64.52% accuracy on $R@1$. This demonstrates that densely sampled data in a single area is harder than data sampled from random areas.

Experiments on Vo (Vo & Hays, 2016): The performance on the Vo (Vo & Hays, 2016) dataset is presented in Table 11. Due to the difficulties of this dataset, such as the limited field of view and the large-scale testing data size, we only present the recall accuracy at top-1%. We observe that the DBL (Vo & Hays, 2016) method achieved nearly 60% on recall accuracy at top-1% and AlignNet (S. Zhu et al., 2021a) boosted the performance to near 90% because of the global hard example sampling strategy and its novel binomial loss function.

Experiments on VIGOR (S. Zhu et al., 2021b): VIGOR (S. Zhu et al., 2021b) is a relatively new dataset. Only four methods reported results

on this dataset which is shown in Table 12. The SAFA+Mining row refers to the SAFA (Shi et al., 2019) model with the global mining strategy proposed by (S. Zhu et al., 2021a). The performance of all methods on same-area settings is better than cross-area settings, since the domain gap between training data and testing data under the same-area protocol is less than under the cross-area protocol. VIGOR (S. Zhu et al., 2021b) outperformed the two SAFA-based methods due to its newly proposed IOU-based loss and offset prediction. Benefiting from the advanced transformer architecture and two-stage training, TransGeo (S. Zhu et al., 2022) brought a large improvement in both same-area and cross-area evaluation.

Experiments on University-1652 (Z. Zheng et al., 2020): Since University-1652 is a drone-view-focused dataset, we only show the benchmark result on drone-aerial pairs in Table 13. The ‘baseline method’ in Table 13 refers to the baseline model proposed by (Z. Zheng et al., 2020). LPN (T. Wang et al., 2021) achieved better results on both recall accuracy at top-1 and AP than all other methods because of its square-ring partitioning strategy and local pattern network.

4.9 Discussion and Future Work

Cross-view image geo-localization has been developing rapidly in recent years because of the accessibility of geo-tagged aerial images. Many recent works take the advantage of these publicly available resources to build large-scale datasets. By leveraging large-scale datasets, deep learning models achieved remarkable results on cross-view image geo-localization. However, future developments in cross-view geo-localization are still achievable in several aspects: 1) Cross-view image geo-localization under low-light environments. 2) Cross-view cross-season image geo-localization.

Current techniques rely on ground-level images which are taken during the daytime. However, one

major application area of cross-view image geo-localization is autonomous vehicles which should operate anytime. The objects in low-light images lose details of contextual information which makes **global representations hard to predict**. To address this problem, future works can employ an image-to-image translation model which converts low-light images into images taken during the daytime. Another solution is to directly use images taken by special sensors which are designed specifically for low illumination conditions, such as Near Infrared (NIR) sensors. However, the loss of color information from infrared sensors can be a problem.

Similar to cross-view image geo-localization under low-light environments, cross-season cross-view image geo-localization can be a practical problem. **Ground images taken in the summer vs the winter have large visual differences due to the heavy snow, ice, and the changes to the trees**. Currently, to the best of our knowledge, no existing dataset collected ground images from the northern area during winter. However, aerial images of such areas are normally captured during the summertime to maximize visibility (most objects are not covered by snow). Thus, there is a need to bridge the temporal domain gap between the ground and aerial images. Future works might solve this problem by using existing domain adaptation methods [H. Xia, Zhao, and Ding \(2021\)](#); [You, Long, Cao, Wang, and Jordan \(2019\)](#). However, there is still a lack of a comprehensive **datasets** for benchmarking purposes.

5 Object Geo-localization

The basic premise behind object geo-localization is to identify, classify, and determine the geolocations of objects visible in images. This technology enables the construction of automated systems that create maps of objects and their locations using only images as input, avoiding the need for hundreds or thousands of hours of human labor. This technology has applications in self-driving cars, automated mapping of roads, asset management and planning, and land surveying ([Chaabane et al., 2021](#); [Nassar, D’Aronco, Lefèvre, & Wegner, 2020](#); [Nassar, Lefevre, & Wegner, 2019](#)).

5.1 Techniques

Object geo-localization can be more thoroughly defined as follows. As input, an algorithm receives

a sequence of consecutive images in the order they were taken, often extracted from a video. Each image in the sequence is commonly referred to as a frame. Each frame is tagged with the GPS coordinates at which it was taken. Depending on the dataset, there may be large discrepancies in the frame rate, camera field of view, and the distance the camera moves between images. In some datasets, each frame may contain images from multiple camera perspectives. Some datasets may have additional metadata associated with each image, such as pose information indicating the 6D orientation of the camera.

As output, a stationary object geo-localization algorithm is expected to produce a single object prediction indicating the GPS position for each object that appears in at least one frame. The key challenge in this task is that each object does not appear in a fixed number of images, so algorithms must be designed to ‘merge’ the repeated occurrences of objects across multiple frames into a single, geo-localized prediction for each ground-truth object. Sometimes, this task involves predicting additional outputs such as a class label or the object’s condition.

We briefly note that there exists a related field, *Single Image Depth Estimation*, in which the goal is to predict a depth value for each pixel within an image. By contrast, object geo-localization algorithms are designed to receive additional camera metadata such as the camera’s heading and GPS coordinates as inputs to the model, which enables global geo-localization by explicitly predicting GPS coordinates for each object. We direct the reader to ([Mertan, Duff, & Unal, 2021](#)) for additional information on depth estimation.

The most defining challenge in the object geo-localization task is the need to develop some sort of algorithm that merges repeated detections for each object into a single prediction per ground truth object. Therefore, we divide the proposed techniques into three categories based on how they handle repeated detections. **Tracker-based** approaches implement an object tracking algorithm to identify the same object across multiple frames to merge them together. **Triangulation-based** approaches implement a triangulation algorithm to find and merge nearby objects. **Re-identification** approaches use an object detector that detects objects by receiving multiple frames as input and implicitly merging repeated detections from the input frames. Next, we introduce each of the above-mentioned concepts in detail and then survey the popular implementations in the field.

5.1.1 Tracker-Based geo-localization

All tracker-based approaches begin with an object detector that receives images as input and produces a detection for each object of interest. This leaves the need to merge repeated detections from objects appearing in multiple frames. Tracker-based approaches solve this problem by implementing an object tracker that performs object tracking by associating objects across frames. A list of assigned detections from a sequence of frames is referred to as a **tracklet**. It contains what is believed by the algorithm to be all the occurrences of the same object. These approaches will typically implement a heuristic approach to condense each tracklet into the final, geolocalized object predictions.

(Chaabane et al., 2021) constructed a three-stage system that was mostly end-to-end trainable. The first stage detected objects, regressed their bounding boxes, and predicted the 5D pose of visible objects as illustrated in Figure 31. An object's 5D pose contains its translation vector along the X, Y, and Z axis as well as its rotation along the two-axis vector orthogonal to the camera. GPS coordinates for an object were predicted by performing a coordinate transformation using the object's 5D pose relative to the camera's GPS coordinates. From each detection, the authors harvested geometric features predicted by the pose network in addition to visual information extracted from a CNN. These features were provided as input to the object matching network, which they trained to compute affinity scores between each possible pair of detected objects between frames. The output of the matching network was a matrix where each entry indicated the predicted similarity between a pair of detections. Finally, the Hungarian algorithm was employed to compute the optimal pairings between objects. The main advantage of this approach is that it is mostly end-to-end trainable. A noteworthy disadvantage is that it requires object 5D poses and the camera intrinsic matrix, which may be unavailable in many applications.

(Wilson et al., 2021) modified the popular object detector RetinaNet (Lin, Goyal, Girshick, He, & Dollár, 2020) with an additional subnet to predict GPS coordinates. They trained a second neural network which was designed to predict similarity scores between each pair of sign detections between consecutive frames. The authors used the Hungarian Algorithm to pair detections of objects across multiple frames. The algorithm was modified with a cutoff

value to prevent traffic signs with low similarity from being paired. Finally, each tracklet obtained through this procedure was condensed into a single geolocalized sign prediction with a simple weighted average. The full pipeline is displayed in Figure 32. Compared to (Chaabane et al., 2021), this approach can be run with more commonly accessible hardware due to not requiring 5D poses, and has the additional capability to predict object classes as part of its geo-localization pipeline. However, the system is more complicated and not end-to-end trainable.

5.1.2 Triangulation-Based Object Geo-localization

Similar to tracker-based approaches, triangulation-based methods use an object detector to provide initial detections for objects in individual frames. However, triangulation approaches use an alternative method for condensing and geo-localizing repeated detections. Triangulation works by first constructing a triangle with three points. In the case of object geo-localization, there would be two points on the triangle corresponding to two camera locations, and then the third point would be the location of the object since it should remain constant between frames. The distance between images can be calculated from GPS metadata, and the angle between the camera and the object can be predicted by the object detection model. This allows the distance to the object to be predicted from this triangle using trigonometry. The calculated distance can serve as a known value in the next triangle, which is constructed by connecting the next frame in the sequence to this edge. This process can be repeated as many times as necessary to connect and merge object detections. In real applications, object positions may be very noisy and the rays drawn from object positions may not always intersect to form a perfect triangle. (R.I. Hartley & Sturm, 1997) proposed a method robust to noise by formulating triangulation as a minimum least squares problem. Note that (R. Hartley & Zisserman, 2003) provides a thorough description of various triangulation and geometric computer vision methods.

In practice, a hybrid approach is typically employed in which triangulation is one of components in a geo-localization pipeline. Krylov, Kenny, and Dahyot (2018) built a complete geo-localization system involving two convolutional networks, the first of which segments objects visible in images, and the second estimates the depth of each detected object. After

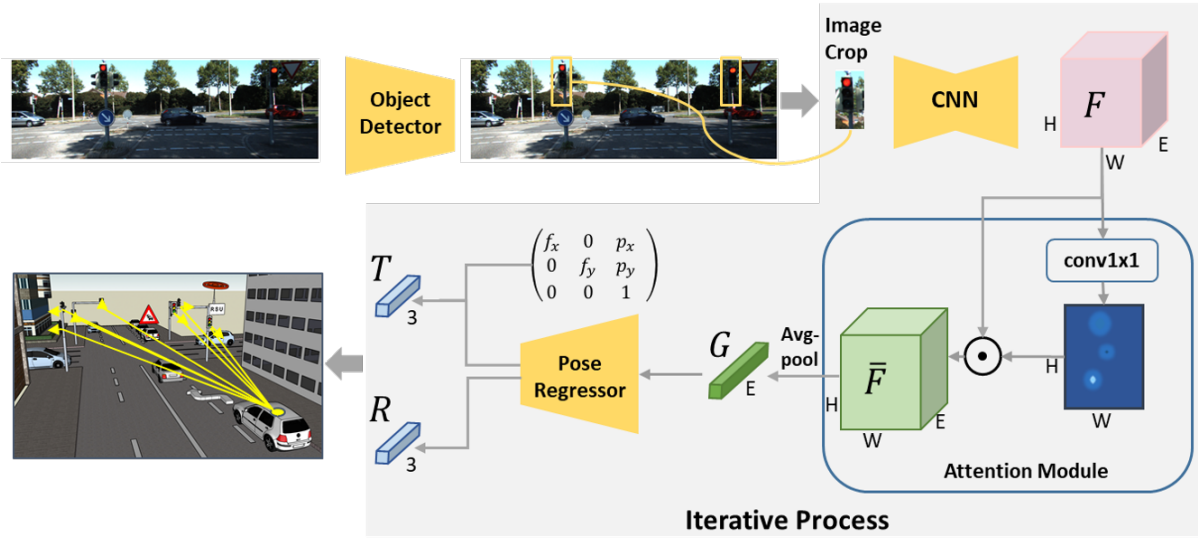


Fig. 31: The object detector proposed by (Chaabane et al., 2021) that regresses 5D poses for objects. The figure is taken from (Chaabane et al., 2021).

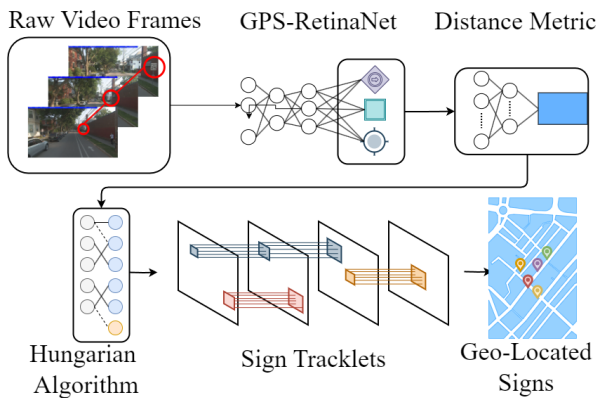


Fig. 32: The full end-to-end system including the object detector and tracker proposed by (Wilson et al., 2021). Figure is taken from (Wilson et al., 2021).

using these networks to detect objects and estimate their depths, objects are geolocated using a Markov Random Field model to perform triangulation. This model optimizes an energy function to yield refined predictions for objects and their geolocation from each pair of images. Since objects are still likely to appear in more than two frames (even after triangulation), the authors filtered the redundant object detections using a hierarchical clustering algorithm. The full pipeline is shown in Figure 33. This approach is conceptually simple and has strong explainability due to the use of **triangulation** to determine GPS coordinates, however,

has less performance than deep learning-based GPS prediction methods.

5.1.3 Re-Identification-Based Object Geolocation

Another approach to address the issue of repeated detections is to inherently detect the object from multiple views. Instead of receiving a single frame as input, a detector receives one or more nearby frames as simultaneous inputs, and learns to jointly predict and re-identify the same object between frames as a single output. By performing detection from multiple perspectives, the object detector implicitly merges repeated detections from multiple frames.

(Nassar et al., 2019) used an approach in which an object's geolocation is predicted using multi-view geometry. The system contained a siamese network that learned to detect, re-identify, and geolocalize objects using a pair of images as simultaneous inputs, as illustrated in Figure 34. After regressing bounding boxes in one image, their model learned a transformation to project those bounding boxes to the perspective of the other image. This gave the model the capability to detect and predict the geolocation of objects by learning the joint distribution from both images. Since only a single prediction is generated for objects appearing in both images, their model implicitly merges detections from each pair of images. This means their model did not require a separate object

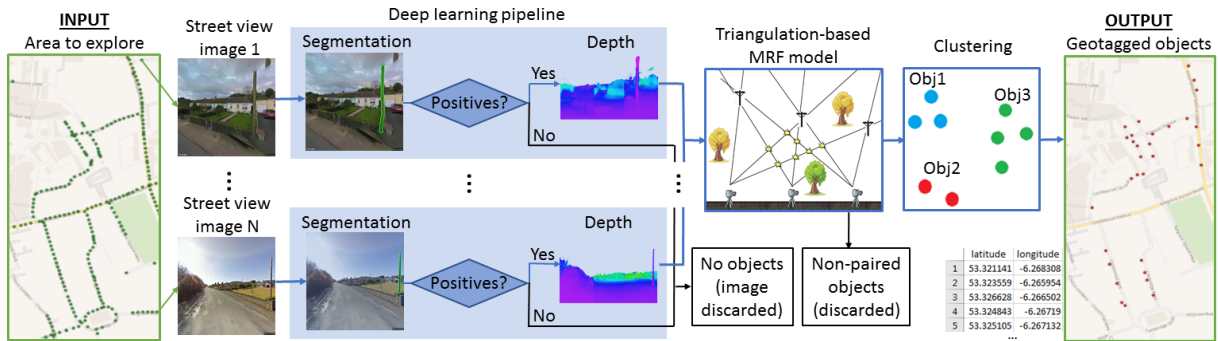


Fig. 33: The full pipeline including the detector, triangulation, and clustering proposed by Krylov et al. (2018). Figure is taken from Krylov et al. (2018).

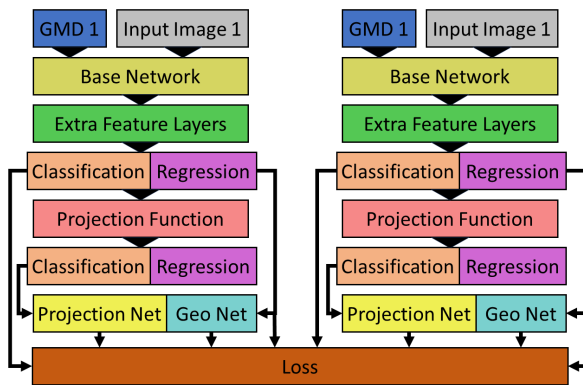


Fig. 34: The siamese network that learns to re-identify objects between a pair of frames proposed by (Nassar et al., 2019). Figure is taken from (Nassar et al., 2019).

tracker to merge repeated detections unlike (Chaabane et al., 2021; Wilson et al., 2021). The limitation of this approach is that it can not collapse redundant detections from objects visible in greater than two frames.

(Nassar et al., 2020) proposed an algorithm capable of geo-localizing objects using an arbitrary number of images as input. First, images were fed into an object detector, from which fused features across all input images were extracted and used to predict bounding boxes and classes for each visible object. To associate detections of the same objects, a graph neural network (GNN) was used. Each node in the graph represents a feature vector corresponding to a proposed object from the detector, and each edge weight encodes if two nodes are from the same object. The GNN was trained to learn weights on the edges, allowing geolocalized object detections to be produced by finding each connected component in the graph. The

proposed architecture is fully end-to-end trainable. Since this approach can merge objects from greater than two images, this approach solves the previous pitfall present in (Nassar et al., 2019).

5.1.4 Other Approaches

Since detecting an object in a satellite image with known coordinates implicitly provides the approximate geolocation of the object, this task could be interpreted as an approximate form of geolocalization. (Shermeyer & Etten, 2019) proposed to enhance satellite image quality using the Very Deep Super-Resolution Network (J. Kim, Lee, & Lee, 2016). They trained object detection models on the xView dataset (Lam et al., 2018) to detect common objects from satellite images such as planes and boats. To reduce the burden of human annotation, (Martinson, Furlong, & Gillies, 2021) proposed a two-step system. First, they generated synthetic satellite images of objects by employing CycleGAN (J.-Y. Zhu, Park, et al., 2017). Second, they trained RetinaNet (Lin et al., 2020) on the xView dataset. Then they used the synthetic images to determine a confidence score threshold to filter detections, which reduced false positives. (G.-S. Xia et al., 2018) provides a modern satellite image object recognition dataset that addresses several issues associated with previous datasets. Specifically, they provide a large number of samples per class and propose a method of drawing bounding boxes to address the overlap typically associated with objects in satellite images. The key disadvantages are that smaller objects such as electric poles may not be visible, and different classes of objects such as traffic signs may not be distinguishable from an aerial perspective.

5.2 Datasets

Multiple datasets have been constructed to benchmark the performance of object geo-localization algorithms. Datasets in this field contain a few common characteristics. First, they all contain frames organized sequentially in the order in which they were taken. Each frame in these datasets has GPS metadata associated with them, which indicates the longitude and latitude at which the frame was captured. Second, all datasets contain per-frame annotations of objects. Each object annotation specifies a bounding box around the object along which either its GPS coordinates or a distance offset relative to the frame that can be used to recover the object's GPS coordinates using a coordinate transform. Third, each dataset needs to have some method of identifying repeated appearances of the same object in multiple frames, to provide the ground truth against which to compare the final geo-localization performance of the algorithm. Many datasets accomplish this with a unique label associated with each annotation, such that the same object will have the same label in each of its annotations. Some datasets provide a list of each of the alternate frames the object appears in as part of the object's annotation. Finally, a few datasets simply assume that all annotations within a certain distance of each other correspond to the same object.

Unlike other fields where datasets contain clearly defined inputs and outputs and existing models can be re-trained on other datasets, the field of object geo-localization is yet to adopt a standardized structure or consistent set of testing datasets. While all datasets contain bounding box and geolocation information associated with each annotation, datasets differ in terms of their annotation structure, available camera metadata, construction techniques, and hardware. Some datasets contain additional metadata such as the camera heading or orientation (also referred to as pose) associated with each image. This may serve as additional input to assist the object detector in identifying objects and predicting geolocation. Finally, datasets are built using different hardware. Many techniques mine publicly available images created with consumer equipment such as GPS-tagged cellphone images, whereas other datasets may be professionally constructed using enterprise cameras and LIDAR sensors. As a result of hardware differences, the resulting datasets have widely varying frame rates, movement speeds, and object sizes and distances from the camera. Some datasets may have multiple camera perspectives as part of a single frame.

Due to these differences in datasets, models in this emerging field are currently not cross-dataset-compatible. Models are typically built to use specific inputs associated with camera metadata or object annotations unique to that dataset, and would need to be restructured significantly to train on other datasets. Approaches therefore construct their own datasets and build their model specifically based on how those datasets are structured. This poses a significant challenge when comparing benchmarks across different datasets, as discussed in 5.3. Next, we will discuss each proposed dataset and provide a link to datasets that are publicly available. In Table 14, we compare the popular single-object geo-localization datasets.

Uber-TL:²⁵ (Chaabane et al., 2021) constructed a dataset in which the objective is to geo-localize traffic lights from images captured from a roadside vehicle. The authors mined their data from nuScenes (Caesar et al., 2020), a pre-existing dataset commonly used for autonomous driving. The authors selected scenes from this dataset containing road intersections with traffic lights within 100 meters of the camera. Object coordinates are expressed relative to the camera's perspective, and each frame contains images from six separate camera angles as the vehicle moves down the road. The total dataset contains 96,960 distinct images.

This dataset contains very accurate GPS locations for traffic lights due to the use of LIDAR. There are many camera angles available providing a wide field-of-view and multiple camera angles for most objects. The images are captured at a high resolution and high frame rate. The limitation of this dataset is that many of these ideal criteria may not be met in real-world settings. For example, it is often unfeasible to capture data at six simultaneous camera angles, especially at a high frames rate due to storage constraints. Traffic signs which were not visible in five distinct keyframes were also removed from the dataset, artificially reducing the difficulty of the dataset relative to real-world settings.

ARTSv2:²⁶ (Wilson et al., 2021) built a dataset of street-view images in which the objective is to classify and geo-localize traffic signs. The dataset contains 199 unique sign classes, 25,544 images containing at

²⁵ https://github.com/MedChaabane/Static_Objects_Geolocalization

²⁶ https://drive.google.com/drive/folders/1u_nx38M0_owB0cR-qA6IOWgZhGpb9sWU?usp=sharing

least one annotation, and 47,589 unique annotations. Each annotation specifies the sign's class, a bounding box around the sign, a unique integer identifier used to indicate the same sign in different images, and attributes specifying which side of the road the sign is placed on and whether it is a part of an assembly. Each image contains camera metadata indicating its heading and geolocation. The strengths of this dataset are that it has a broad and imbalanced distribution of classes and a variety of different environments, which is very representative of what a geo-localization model would encounter in the real world. Its limitations are noisy GPS coordinates and potentially inconsistent class labels due to the use of human annotators.

MRF-TLG: Krylov et al. (2018) constructed two datasets. First, they built a traffic light dataset (different from (Chaabane et al., 2021)) using data samples mined from Mapillary vistas (Neuhold, Ollmann, Bulò, & Kontschieder, 2017) and Cityscapes (Cordts et al., 2016). In total, the dataset contains around 18,500 images scaled to 640×640 resolution. The main limitation of this dataset is that objects within one meter are assumed to be the same object. This could be considered a fairly generous assumption, since many separate traffic lights are commonly placed on the same pole, and scenarios in which objects are close together are most challenging.

MRF-TP: The second dataset created by (Krylov et al., 2018) contains 20,000 images of telephone poles and 15,000 Google Street View (GSV) images. The authors note that the GPS coordinates are very inaccurate in this dataset due to inconsistent coordinate labels for the GSV images combined with objects being frequently blocked.

PMV: (Nassar et al., 2019) constructed two datasets. First, they created the Pasadena Multi-View Re-Identification dataset containing streetside trees (Nassar et al., 2019). This dataset contains 6,020 trees labeled in 6,141 panoramas taken from Google Street View (GSV). Each tree appears in exactly four panoramas, leaving a total of 25,061 bounding boxes indicating the location of trees. Each annotation provides the geo-location of the tree, and a unique identifier distinguishing it from other trees. Camera locations are also available in each image as metadata. The main limitation of this dataset is that each tree appears in exactly four images, and the images selected to be part of the dataset are those for which

the tree is closest to the camera. This is a significant limitation since closer objects are far easier to geo-localize, artificially making the task less difficult than real-world applications.

GeoSign: (Nassar et al., 2019) built a second dataset sourced from Mapillary (Neuhold et al., 2017) involving traffic signs. This dataset contains 31,442 traffic signs and a total of 74,320 images. Each annotation specifies the sign's geolocation and altitude, a polygon surrounding the sign, and a list of images in which the sign appears. Camera location metadata is also available for each image. The main limitation of this dataset is inconsistencies in image quality and resolution, due to the crowd-sourced nature of the dataset.

5.3 Performance Benchmarks

We would like to preface this topic by emphasizing the caveat on performance metrics in this field. First, there are no standard performance metrics agreed upon to evaluate algorithms across this field. Second, the method to compute true positives, false positives, false negatives, and the distribution of distance errors differ between different approaches, mainly due to differences in dataset construction techniques. Some methods count all nearby objects within a certain distance threshold as a single object. Other methods ignore objects outside of a certain distance from the camera during evaluation. Due to the lack of standard test datasets and performance metrics, we can not perform a direct side-by-side comparison between the proposed methods. Therefore, we list each algorithm, the datasets it was benchmarked on, and provide details of how the evaluation was performed. A summary of the results is provided in Table 15.

Chaabane et al. (2021) benchmarked on the traffic light dataset they constructed themselves. Since their system contains both a 5D pose regression network and an object detector, they provided separate benchmarks for the performance of each component. To benchmark the 5D pose network, the authors reported the translation and rotational error for both objects within 20 meters and for all objects at any distance. They reported average margins of error of 2.51 meters and 14.21 deg for objects within 20 meters, and 4.43 meters and 15.97 deg for objects at any distance. They analyzed the tracker's performance on their dataset using the Multiple Object Tracking Accuracy (MOTA) metric and reported a score of 85.52%. To benchmark

	PMV (Nassar et al., 2019)	TLG (Chaabane et al., 2021)	ARTS v1.0 (Almutairy et al., 2021)		ARTS v2 (Wilson et al., 2021)
			EASY	CHALLENGING	
Number of classes	1	1	62	175	199
Number of images	6141	96960	6807	16023	25544
Number of annotations	25061	N/A	9006	27181	47589
Side of the road					✓
Assembly					✓
Unique Object IDs	✓	✓			✓
5D Poses		✓			
GPS	✓	✓	✓	✓	✓
Color Channels	RGB	RGB	RGB	RGB	RGB
Image Resolution	2048 × 1024	1600 × 1900	1920 × 1080	1920 × 1080	1920 × 1080
Publicly Available		✓	✓	✓	✓

Table 14: A comparison of the characteristics of popular single-object geo-localization datasets. Table is taken from (Wilson et al., 2021).

geo-localization performance, the authors defined a true positive as a traffic light prediction within 2 meters of Euclidean distance or 3 meters of Mahalanobis distance of the ground truth. They provided precision-recall curves for both units of measurement. The approximate precision-recall values from the ‘elbows’ of the PR curves were 0.75 and 0.45, and 0.85 and 0.55 when using Euclidean and Mahalanobis distances respectively.

(Wilson et al., 2021) benchmarked a dataset they constructed using US traffic signs. Because the dataset contains hand-labeled annotations from low frame-rate videos, GPS noise is likely to be greater than other methods. They defined a true positive to be a scenario in which the geo-localization error plus a class mismatch penalty is less than 15 meters. They provided separate benchmarks for their object tracker and geo-localization performance. The authors reported an object detection mean average precision (mAP) of 0.701. When benchmarking geo-localization performance using the aforementioned definition of true positives, the authors reported a precision and recall of 0.81 and 0.708 respectively.

(Nassar et al., 2019) benchmarked their performance on both the datasets they constructed, one of which contained trees and the other contained traffic signs. Note that this dataset does not involve sign classification. The authors reported multi-view re-identification results of 0.731 and 0.882 with mean average geo-localization errors of 3.13 and 4.36 on the respective datasets. The same two datasets were used to benchmark the multi-view re-identification performance of the graph neural network proposed in (Nassar et al., 2020). When performing re-identification from six views, they reported a mean average precision of 0.763 and 0.924 and mean geo-localization errors in meters of 2.75 and 4.21 on the respective datasets.

(Krylov et al., 2018) tested their triangulation-based approach on the two datasets they constructed containing traffic lights and telegraph poles. They benchmarked their detector by first segmenting the pixels of objects in the image. They defined a true positive to be a scenario in which the segmentation network correctly labeled over 25% of the object’s pixels. Objects greater than 25 meters from the camera were ignored since they would cause a large performance drop.

Using this method, they reported precision and recall values of 0.951 and 0.981 respectively on their traffic light dataset and 0.979 and 0.927 respectively on their telegraph pole dataset. To evaluate geo-localization performance, the authors defined a true positive as a situation in which a predicted object was within 2 meters of the ground truth. An important limitation to be noted is that annotated objects within 1 meter were assumed to be the same object. Using these definitions, the authors reported precision and recall values of 0.940 and 0.922 respectively on their traffic light dataset and 0.926 and 0.973 respectively on their telegraph pole dataset. They reported 95th percentile geo-localization margins of error of 1.89 and 2.07 meters on the respective datasets.

5.4 Discussion and Future Work

Object geo-localization is a rising field with broad applicability to a very practical set of problems. One advantage of this field is that there is an enormous amount of geotagged images that can be mined from the internet, especially since modern smartphones embed GPS coordinates in an image's EXIF data. Unfortunately, annotation can be challenging and inconsistent which is currently the largest shortcoming in the field. In the future, researchers may consider developing semi-supervised approaches to reduce the large annotation burden in this field. Similarly, the field needs to accept standardized datasets and performance metrics so that different methods can be properly compared. Researchers should also consider collecting datasets from more diverse environments, as most current datasets are limited to various road assets. Land surveying, for example, is a domain that is currently under-represented. These algorithms are particularly **applicable in** less developed countries where assets are less managed, creating demand for automated tools. Future research could address this demand by enhancing algorithm performance on low-resolution images, and making algorithms robust to work on smaller datasets and in cross-dataset settings.

6 Conclusion

In this paper, we surveyed noteworthy approaches within the broad field of geo-localization involving images and objects within these images. We divided geo-localization into three key sub-fields.

Single-view geo-localization approaches attempt to predict GPS coordinates taken from a single perspective. A simple approach to accomplish this task is to divide the surface of the earth into cells and which enables the formulation geo-localization as a classification problem in which the goal is to classify which cell an image originates from. The greatest strength of these approaches is their simplicity. Because classification is already a well understood and thoroughly studied problem in machine learning, existing classification models can be easily adapted to this solution. However, the accuracy of these predictions is limited based on the size of the divided cells, and division into smaller cells results in fewer training samples per class. An alternative approach is to match a query image against a similar image from a reference database with known coordinates. This allows for a direct prediction of GPS coordinates as opposed to limiting geospatial predictions to an approximate cell. The main disadvantage of this approach is that as the size of the reference database grows, the number of images against which the query must be compared increases which can become computationally prohibitive. It is also challenging to extract features that match the query to reference images regardless of illumination, camera angle, vegetation, etc. A less popular technique involves refining pre-existing GPS coordinates instead of predicting them from scratch. These approaches can achieve greater performance by using the pre-existing coordinates as a starting prediction, but the obvious disadvantage is these approaches require that GPS coordinates are already available. A final class of approaches involves geo-localizing rural images by aligning their skyline features with a digital elevation model. These approaches have the capability to geo-localize images in rural environments where fewer descriptive features are available, but their performance is limited due to the more difficult task formulation.

All single-view methods are inherently restricted in their capabilities due to only receiving a single ground image perspective as input. Cross-view approaches were designed to address these limitations by incorporating aerial images to increase performance. In cross-view geo-localization, a database of satellite imagery is incorporated to more robustly determine the location of ground-view imagery. Joint feature extraction methods aim to extract hand-crafted features that are similar for ground and satellite images from the same location. These methods are able to exploit a large database of satellite imagery,

Method	Technique	Dataset	Mean GPS Error (m)	Precision	Recall	MAP
UBER-NET Chaabane et al. (2021)	Tracker-Based	TLG Chaabane et al. (2021)	4.43	0.75 ¹	0.45 ¹	0.928
GPS-RetinaNet Wilson et al. (2021)	Tracker-Based	ARTSv2 Wilson et al. (2021)	5.81	0.810	0.708	0.701
Multi-View Nassar et al. (2019)	Re-Identification	PMV Nassar et al. (2019)	3.13	N/A	N/A	0.731
Multi-View Nassar et al. (2019)	Re-Identification	Mapillary TLG Nassar et al. (2019)	4.36	N/A	N/A	0.882
GeoGraph Nassar et al. (2020)	Re-Identification	PMV Nassar et al. (2019)	2.75	N/A	N/A	0.763
GeoGraph Nassar et al. (2020)	Re-Identification	Mapillary TLG Nassar et al. (2019)	4.21	N/A	N/A	0.924
MRF Krylov et al. (2018)	Triangulation	Traffic Lights 2 Krylov et al. (2018)	1.89 (95th percentile)	0.922	0.940	N/A
MRF Krylov et al. (2018)	Triangulation	Telegraph Poles Krylov et al. (2018)	0.98	0.973	0.926	N/A

Table 15: A comparison of performance metrics reported by different stationary object geo-localization algorithms. Note that the structure of the datasets and the performance evaluation methods

differ drastically. Values marked ¹ are approximate values taken from the "elbow" of the graph illustrating the precision-recall curve.

but their capabilities are limited by their use of hand-crafted features. To address this limitation, Siamese network approaches were developed to automatically learn features to associate ground and satellite images from the same location. These methods do not, however, explicitly model objects such as trees and buildings visible in an image. To accomplish this, graph-based approaches were proposed in which each landmark from an image was modeled with a node, and the connectivity between landmarks was modeled with an edge. This problem formulation yields greater interpretability than other approaches. All of these approaches, however, suffer from the issue of losing certain low-level features present in ground-view images. A final approach leverages generative models to create artificial ground-view images, which can then be directly matched against real ground-view images to perform geo-localization. This process trains a model to directly convert aerial to ground images thus maintaining as many features as the model is capable of. The primary disadvantage is the reliance on GANs, which are known to be difficult to work with.

A limitation of both single and cross-view approaches is that they are exclusively designed for the task of predicting image locations. Object geo-localization algorithms were designed to instead geo-localize objects visible within the images. These approaches are differentiated by the methods they use to condense repeated detections of the same object. Triangulation approaches use changes in camera and object depth to triangulate object positions. These approaches are conceptually simplistic, but they rely on precise camera parameters to be accurate, and typically require a separate algorithm (such as clustering) to completely condense repeated detections. Tracker-based approaches attempt to track the position of the same object between images. These approaches have

high performance but require that the **input** images are sequential. Re-identification approaches build detection models that receive multiple images as input to produce a single output detection, which implicitly merges the repeated occurrences of objects across the input images. These approaches fail, however, if an object doesn't appear in enough input images for the detector. Furthermore, the detectors only merge objects from a fixed number of images.

Advancements in machine learning, computer vision, and available hardware provide continual opportunities to improve the state-of-the-art in image geo-localization. Future research can focus on the use of self-supervised learning to extract more powerful features from deep learning models. Transformer architectures (Vaswani et al., 2017) have recently been adapted for image processing tasks and in many cases are out performing convolutional networks. Applying modern vision transformers to image geo-localization problems has the potential to further improve the state-of-the-art in the field. Due to the amounts of data required by deep learning models, larger and higher quality datasets could further enhance results. Since applications for image geo-localization commonly **involve** user created imagery, continued research should be applied to building algorithms that are not reliant on specific illumination, vegetation, camera perspectives, or other consistent conditions. Instead, models must be trained to extract features invariant of the inconsistencies associated with crowd sourced datasets.

Declarations

The authors have no competing interests to declare that are relevant to the content of this article.

References

- Agarwal, S., Furukawa, Y., Snavely, N., Simon, I., Curless, B., Seitz, S.M., Szeliski, R. (2011, October). Building rome in a day. *Commun. ACM*, 54(10), 105–112.
doi:<https://doi.org/10.1145/2001269.2001293>
- Almutairy, F., Alshaabi, T., Nelson, J., Wshah, S. (2021). Arts: Automotive repository of traffic signs for the united states. *Institute of Electrical and Electronics Engineers (IEEE) Transactions on Intelligent Transportation Systems*, 22(1), 457-465.
doi:<https://doi.org/10.1109/TITS.2019.2958486>
- Anguelov, D., Dulong, C., Filip, D., Frueh, C., Lafon, S., Lyon, R., ... Weaver, J. (2010). Google street view: Capturing the world at street level. *Institute of Electrical and Electronics Engineers (IEEE) Computer*, 43(6), 32-38.
doi:<https://doi.org/10.1109/MC.2010.170>
- Ankerst, M., Breunig, M.M., Kriegel, H.-P., Sander, J. (1999). Optics: Ordering points to identify the clustering structure. *Proceedings of the 1999 acm sigmod international conference on management of data* (p. 49–60). New York, NY, USA: Association for Computing Machinery. Retrieved from <https://doi.org/10.1145/304182.304187>
doi:<https://doi.org/10.1145/304182.304187>
- Arandjelović, R., Gronat, P., Torii, A., Pajdla, T., Sivic, J. (2018). Netvlad: Cnn architecture for weakly supervised place recognition. *Institute of Electrical and Electronics Engineers (IEEE) Transactions on Pattern Analysis and Machine Intelligence (TPAMI)*, 40(6), 1437-1451.
doi:<https://doi.org/10.1109/TPAMI.2017.2711011>
- Baatz, G., Saurer, O., Köser, K., Pollefeys, M. (2012). Large scale visual geo-localization of images in mountainous terrain. A. Fitzgibbon, S. Lazebnik, P. Perona, Y. Sato, & C. Schmid (Eds.), *Computer vision – eccv 2012* (pp. 517–530). Berlin, Heidelberg: Springer Berlin Heidelberg.
- Baatz, G., Saurer, O., Köser, K., Pollefeys, M. (2012, 10). Leveraging topographic maps for image to terrain alignment. (p. 487-492). doi:<https://doi.org/10.1109/3DIMPVT.2012.33>
- Bansal, M., & Daniilidis, K. (2014). Geometric urban geo-localization. *Institute of electrical and electronics engineers (ieee) conference on computer vision and pattern recognition (cvpr)* (p. 3978-3985). doi:<https://doi.org/10.1109/CVPR.2014.508>
- Benbihi, A., Arravechia, S., Geist, M., Pradalier, C. (2020, 05). Image-based place recognition on bucolic environment across seasons from semantic edge description. (p. 3032-3038). doi:<https://doi.org/10.1109/ICRA40945.2020.9197529>
- Brejcha, J., & Cadik, M. (2017, 06). Geopose3k: Mountain landscape dataset for camera pose estimation in outdoor environments. *Image and Vision Computing*, 66.
doi:<https://doi.org/10.1016/j.imavis.2017.05.009>
- Brejcha, J., & Čadík, M. (2017). State-of-the-art in visual geo-localization. *Pattern Analysis and Applications*, 20(3), 613–637.
- Brejcha, J., Lukáč, M., Chen, Z., DiVerdi, S., Čadík, M. (2018). Immersive trip reports. *Proceedings of the 31st annual acm symposium on user interface software and technology* (p. 389–401). New York, NY, USA: Association for Computing Machinery. Retrieved from <https://doi.org/10.1145/3242587.3242653>
doi:<https://doi.org/10.1145/3242587.3242653>
- Brejcha, J., Lukáč, M., Hold-Geoffroy, Y., Wang, O., Cadik, M. (2020, 10). Landscapear: Large scale outdoor augmented reality by matching photographs with terrain models using learned descriptors. In (p. 295-312). doi:https://doi.org/10.1007/978-3-030-58526-6_18

- Brock, A., Donahue, J., Simonyan, K. (2019). Large scale GAN training for high fidelity natural image synthesis. *International conference on learning representations (iclr)*.
- Bromley, J., Bentz, J.W., Bottou, L., Guyon, I., LeCun, Y., Moore, C., ... Shah, R. (1993). Signature verification using a “siamese” time delay neural network. *International Journal of Pattern Recognition and Artificial Intelligence (IJPRAI)*, 7(04), 669–688.
- Caesar, H., Bankiti, V., Lang, A.H., Vora, S., Liong, V.E., Xu, Q., ... Beijbom, O. (2020). nuscenes: A multimodal dataset for autonomous driving. *Institute of Electrical and Electronics Engineers (IEEE)/CVF Conference on Computer Vision and Pattern Recognition (CVPR)*, 11618-11628.
- Cai, S., Guo, Y., Khan, S., Hu, J., Wen, G. (2019, October). Ground-to-aerial image geo-localization with a hard exemplar reweighting triplet loss. *Proceedings of the institute of electrical and electronics engineers (ieee)/cvf international conference on computer vision (iccv)*.
- Castaldo, F., Zamir, A., Angst, R., Palmieri, F., Savarese, S. (2015, December). Semantic cross-view matching. *Proceedings of the institute of electrical and electronics engineers (ieee) international conference on computer vision (iccv) workshops*.
- Chaabane, M., Gueguen, L., Trabelsi, A., Beveridge, R., O’Hara, S. (2021, January). End-to-end learning improves static object geo-localization from video. *Proceedings of the ieee/cvf winter conference on applications of computer vision (wacv)* (p. 2063-2072).
- Chen, D.M., Baatz, G., Köser, K., Tsai, S.S., Vedantham, R., Pylvänäinen, T., ... Grzeszczuk, R. (2011). City-scale landmark identification on mobile devices. *Computer vision and pattern recognition (cvpr)* (p. 737-744). doi:<https://doi.org/10.1109/CVPR.2011.5995610>
- Chen, W., Liu, Y., Wang, W., Bakker, E., Georgiou, T., Fieguth, P., ... Lew, M. (2021, 01). *Deep image retrieval: A survey*.
- Chen, Y., Qian, G., Gunda, K., Gupta, H., Shafique, K. (2015). Camera geolocation from mountain images. *18th International Conference on Information Fusion (Fusion)*, 1587-1596.
- Chopra, S., Hadsell, R., LeCun, Y. (2005). Learning a similarity metric discriminatively, with application to face verification. *Institute of electrical and electronics engineers (ieee) computer society conference on computer vision and pattern recognition (cvpr)* (Vol. 1, pp. 539–546).
- Clark, B., Kerrigan, A., Kulkarni, P., Cepeda, V., Shah, M. (2023, 03). *Where we are and what we’re looking at: Query based worldwide image geo-localization using hierarchies and scenes*. doi:<https://doi.org/10.48550/arXiv.2303.04249>
- Cordts, M., Omran, M., Ramos, S., Rehfeld, T., Enzweiler, M., Benenson, R., ... Schiele, B. (2016, June). The cityscapes dataset for semantic urban scene understanding. *Proceedings of the institute of electrical and electronics engineers (ieee) conference on computer vision and pattern recognition (cvpr)*.
- Costea, D., & Leordeanu, M. (2016, September). Aerial image geolocation from recognition and matching of roads and intersections. E.R.H. Richard C. Wilson & W.A.P. Smith (Eds.), *Proceedings of the british machine vision conference (bmvc)* (p. 118.1-118.12). BMVA Press. doi:<https://doi.org/10.5244/C.30.118>
- Cuturi, M. (2013). Sinkhorn distances: Lightspeed computation of optimal transport. *Advances in neural information processing systems (NeurIPS)*, 26, 2292–2300.
- Dalal, N., & Triggs, B. (2005). Histograms of oriented gradients for human detection. *Institute of electrical and electronics engineers (ieee) computer society conference on computer vision and pattern recognition (cvpr)* (Vol. 1, pp. 886–893).

- Deng, J., Dong, W., Socher, R., Li, L.-J., Li, K., Fei-Fei, L. (2009). Imagenet: A large-scale hierarchical image database. *Institute of electrical and electronics engineers (ieee) conference on computer vision and pattern recognition (cvpr)* (pp. 248–255).
- Dünser, A., Billingham, M., Wen, J., Lehtinen, V., Nurminen, A. (2012). Exploring the use of handheld ar for outdoor navigation. *Computers & Graphics*, 36(8), 1084–1095.
- Fu, C., Xiang, C., Wang, C., Cai, D. (2019, January). Fast approximate nearest neighbor search with the navigating spreading-out graph. *Proc. VLDB Endow.*, 12(5), 461–474.
doi:<https://doi.org/10.14778/3303753.3303754>
- Gao, X., Shen, S., Hu, Z., Wang, Z. (2019). Ground and aerial meta-data integration for localization and reconstruction: A review. *Pattern Recognition Letters*, 127, 202-214. (Advances in Visual Correspondence: Models, Algorithms and Applications (AVC-MAA))
doi:<https://doi.org/https://doi.org/10.1016/j.patrec.2018.07.036>
- Geiger, A., Lenz, P., Stiller, C., Urtasun, R. (2013). Vision meets robotics: The kitti dataset. *International Journal of Robotics Research (IJRR)*.
- Girshick, R. (2015). Fast r-cnn. *Proceedings of the institute of electrical and electronics engineers (ieee) international conference on computer vision (iccv)* (pp. 1440–1448).
- Goodfellow, I., Pouget-Abadie, J., Mirza, M., Xu, B., Warde-Farley, D., Ozair, S., ... Bengio, Y. (2014). Generative adversarial nets. *Advances in neural information processing systems (NeurIPS)*, 27.
- Gu, Y., Wang, Y., Li, Y. (2019). A survey on deep learning-driven remote sensing image scene understanding: Scene classification, scene retrieval and scene-guided object detection. *Applied Sciences*, 9(10).
doi:<https://doi.org/10.3390/app9102110>
- Haas, L., Alberti, S., Skreta, M. (2023, 07). *Pigeon: Predicting image geolocations*.
- Hadsell, R., Chopra, S., LeCun, Y. (2006). Dimensionality reduction by learning an invariant mapping. *Institute of electrical and electronics engineers (ieee) computer society conference on computer vision and pattern recognition (cvpr)* (Vol. 2, pp. 1735–1742).
- Hakeem, A., Vezzani, R., Shah, M., Cucchiara, R. (2006). Estimating geospatial trajectory of a moving camera. *18th international conference on pattern recognition (icpr)* (Vol. 2, p. 82-87). doi:<https://doi.org/10.1109/ICPR.2006.499>
- Hartley, R., & Zisserman, A. (2003). *Multiple view geometry in computer vision* (2nd ed.). New York, NY, USA: Cambridge University Press.
- Hartley, R.I., & Sturm, P. (1997). Triangulation. *Computer Vision and Image Understanding*, 68(2), 146-157. Retrieved from <https://www.sciencedirect.com/science/article/pii/S1077314>
doi:<https://doi.org/https://doi.org/10.1006/cviu.1997.0547>
- Hays, J., & Efros, A. (2015, 10). Large-scale image geolocalization. *Multimodal Location Estimation of Videos and Images*, 41-62.
doi:https://doi.org/10.1007/978-3-319-09861-6_3
- Hays, J., & Efros, A.A. (2008). im2gps: estimating geographic information from a single image. *Proceedings of the institute of electrical and electronics engineers (ieee) conference on computer vision and pattern recognition (cvpr)*.
- Hu, S., Feng, M., Nguyen, R.M., Lee, G.H. (2018). Cvm-net: Cross-view matching network for image-based ground-to-aerial geo-localization. *Proceedings of the institute of electrical and electronics engineers (ieee) conference on computer vision and pattern recognition (cvpr)* (pp.

7258–7267).

- Isola, P., Zhu, J.-Y., Zhou, T., Efros, A.A. (2017, July). Image-to-image translation with conditional adversarial networks. *Proceedings of the institute of electrical and electronics engineers (ieee) conference on computer vision and pattern recognition (cvpr)*.
- Jégou, H., Douze, M., Schmid, C., Pérez, P. (2010). Aggregating local descriptors into a compact image representation. *Institute of electrical and electronics engineers (ieee) computer society conference on computer vision and pattern recognition (cvpr)* (p. 3304-3311). doi:<https://doi.org/10.1109/CVPR.2010.5540039>
- Kalogerakis, E., Vesselova, O., Hays, J., Efros, A.A., Hertzmann, A. (2009). Image sequence geolocation with human travel priors. *Institute of Electrical and Electronics Engineers (IEEE) 12th International Conference on Computer Vision (ICCV)*, 253-260.
- Karras, T., Laine, S., Aila, T. (2019, June). A style-based generator architecture for generative adversarial networks. *Proceedings of the institute of electrical and electronics engineers (ieee)/cvf conference on computer vision and pattern recognition (cvpr)*.
- Kendall, A., & Cipolla, R. (2016). Modelling uncertainty in deep learning for camera relocalization. *Institute of electrical and electronics engineers (ieee) international conference on robotics and automation (icra)* (p. 4762-4769). doi:<https://doi.org/10.1109/ICRA.2016.7487679>
- Kim, D.-K., & Walter, M.R. (2017). Satellite image-based localization via learned embeddings. *Institute of electrical and electronics engineers (ieee) international conference on robotics and automation (icra)* (p. 2073-2080). doi:<https://doi.org/10.1109/ICRA.2017.7989239>
- Kim, H.J., Dunn, E., Frahm, J.-M. (2015). Predicting good features for image geo-localization using per-bundle vlad. *Institute of electrical and electronics engineers (ieee) international conference on computer vision (iccv)* (p. 1170-1178). doi:<https://doi.org/10.1109/ICCV.2015.139>
- Kim, H.J., Dunn, E., Frahm, J.-M. (2017). Learned contextual feature reweighting for image geo-localization. *Institute of electrical and electronics engineers (ieee) conference on computer vision and pattern recognition (cvpr)* (p. 3251-3260). doi:<https://doi.org/10.1109/CVPR.2017.346>
- Kim, J., Lee, J.K., Lee, K.M. (2016). Accurate image super-resolution using very deep convolutional networks. *2016 ieee conference on computer vision and pattern recognition (cvpr)* (p. 1646-1654). doi:<https://doi.org/10.1109/CVPR.2016.182>
- Knight, P.A. (2008). The sinkhorn–knopp algorithm: convergence and applications. *SIAM Journal on Matrix Analysis and Applications*, 30(1), 261–275.
- Krizhevsky, A., Sutskever, I., Hinton, G.E. (2012). Imagenet classification with deep convolutional neural networks. *Advances in neural information processing systems (NeurIPS)*, 25, 1097–1105.
- Krylov, V.A., Kenny, E., Dahyot, R. (2018). Automatic discovery and geotagging of objects from street view imagery. *Remote Sensing*, 10(5). doi:<https://doi.org/10.3390/rs10050661>
- Lam, D., Kuzma, R., McGee, K., Dooley, S., Laielli, M., Klaric, M.K., ... McCord, B. (2018). xvview: Objects in context in overhead imagery. *ArXiv, abs/1802.07856*.
- Lazebnik, S., Schmid, C., Ponce, J. (2006). Beyond bags of features: Spatial pyramid matching for recognizing natural scene categories. *Institute of electrical and electronics engineers (ieee) computer society conference on computer vision and pattern recognition (cvpr)* (Vol. 2, p. 2169-2178). doi:<https://doi.org/10.1109/CVPR.2006.68>

- Lecun, Y., Bottou, L., Bengio, Y., Haffner, P. (1998). Gradient-based learning applied to document recognition. *Proceedings of the IEEE*, 86(11), 2278-2324.
- doi:<https://doi.org/10.1109/5.726791>
- Ledig, C., Theis, L., Huszar, F., Caballero, J., Cunningham, A., Acosta, A., ... Shi, W. (2017, July). Photo-realistic single image super-resolution using a generative adversarial network. *Proceedings of the institute of electrical and electronics engineers (ieee) conference on computer vision and pattern recognition (cvpr)*.
- Lin, T.-Y., Belongie, S., Hays, J. (2013, June). Cross-view image geolocalization. *Proceedings of the institute of electrical and electronics engineers (ieee) conference on computer vision and pattern recognition (cvpr)*.
- Lin, T.-Y., Cui, Y., Belongie, S., Hays, J. (2015, June). Learning deep representations for ground-to-aerial geolocalization. *Proceedings of the institute of electrical and electronics engineers (ieee) conference on computer vision and pattern recognition (cvpr)*.
- Lin, T.-Y., Goyal, P., Girshick, R., He, K., Dollár, P. (2020). Focal loss for dense object detection. *Institute of Electrical and Electronics Engineers (IEEE) Transactions on Pattern Analysis and Machine Intelligence (PAMI)*, 42(2), 318-327.
- doi:<https://doi.org/10.1109/TPAMI.2018.2858826>
- Liu, L., & Li, H. (2019, June). Lending orientation to neural networks for cross-view geolocalization. *Proceedings of the institute of electrical and electronics engineers (ieee)/cvf conference on computer vision and pattern recognition (cvpr)*.
- Lowe, D.G. (2004, November). Distinctive Image Features from Scale-Invariant Keypoints. *International Journal of Computer Vision (IJCV)*, 60(2), 91-110.
- doi:<https://doi.org/10.1023/B:VISI.0000029664.99615.94>
- Lu, X., Li, Z., Cui, Z., Oswald, M.R., Pollefeys, M., Qin, R. (2020, June). Geometry-aware satellite-to-ground image synthesis for urban areas. *Proceedings of the institute of electrical and electronics engineers (ieee)/cvf conference on computer vision and pattern recognition (cvpr)*.
- Martinson, E., Furlong, B., Gillies, A. (2021). Training rare object detection in satellite imagery with synthetic gan images. *2021 institute of electrical and electronics engineers (ieee) /cvf conference on computer vision and pattern recognition workshops (cvprw)* (p. 2763-2770). doi:<https://doi.org/10.1109/CVPRW53098.2021.00311>
- Masone, C., & Caputo, B. (2021). A survey on deep visual place recognition. *IEEE Access*, 9, 19516-19547.
- doi:<https://doi.org/10.1109/ACCESS.2021.3054937>
- Matas, J., Chum, O., Urban, M., Pajdla, T. (2004). Robust wide-baseline stereo from maximally stable extremal regions. *Image and Vision Computing*, 22(10), 761-767. (British Machine Vision Computing 2002)
- doi:<https://doi.org/https://doi.org/10.1016/j.imavis.2004.02.006>
- McManus, C., Churchill, W., Maddern, W., Stewart, A.D., Newman, P. (2014). Shady dealings: Robust, long-term visual localisation using illumination invariance. *Institute of electrical and electronics engineers (ieee) international conference on robotics and automation (icra)* (p. 901-906). doi:<https://doi.org/10.1109/ICRA.2014.6906961>
- Mertan, A., Duff, D.J., Unal, G. (2021). Single image depth estimation: An overview. *ArXiv, abs/2104.06456*.
- Middelberg, S., Sattler, T., Untzelmann, O., Kobbelt, L. (2014). Scalable 6-dof localization on mobile devices. D. Fleet, T. Pajdla, B. Schiele, & T. Tuytelaars (Eds.), *European conference on computer vision (eccv)* (pp. 268-283). Cham:

Springer International Publishing.

- Mirza, M., & Osindero, S. (2014). Conditional generative adversarial nets. *arXiv preprint arXiv:1411.1784*.
- Muller-Budack, E., Pustu-Iren, K., Ewerth, R. (2018, September). Geolocation estimation of photos using a hierarchical model and scene classification. *Proceedings of the european conference on computer vision (eccv)*.
- Narzt, W., Pomberger, G., Ferscha, A., Kolb, D., Müller, R., Wieghardt, J., ... Lindinger, C. (2006). Augmented reality navigation systems. *Universal Access in the Information Society (UAIS)*, 4(3), 177–187.
- Nassar, A.S., D’Aronco, S., Lefèvre, S., Wegner, J.D. (2020). Geograph: Graph-based multi-view object detection with geometric cues end-to-end. A. Vedaldi, H. Bischof, T. Brox, & J.-M. Frahm (Eds.), *European conference on computer vision (eccv)* (pp. 488–504). Cham: Springer International Publishing.
- Nassar, A.S., Lefevre, S., Wegner, J.D. (2019, October). Simultaneous multi-view instance detection with learned geometric soft-constraints. *Proceedings of the ieee/cvf international conference on computer vision (iccv)*.
- Neuhold, G., Ollmann, T., Bulò, S.R., Kotschieder, P. (2017). The mapillary vistas dataset for semantic understanding of street scenes. *Institute of electrical and electronics engineers (ieee) international conference on computer vision (iccv)* (p. 5000-5009). doi:<https://doi.org/10.1109/ICCV.2017.534>
- Oliva, A., & Torralba, A. (2001). Modeling the shape of the scene: A holistic representation of the spatial envelope. *International Journal of Computer Vision (IJCV)*, 42(3), 145–175.
- Pavan, M., & Pelillo, M. (2003). A new graph-theoretic approach to clustering and segmentation. *Institute of electrical and electronics engineers (ieee) computer society conference on computer vision and pattern recognition (cvpr)* (Vol. 1, p. I-I). doi:<https://doi.org/10.1109/CVPR.2003.1211348>
- Pavan, M., & Pelillo, M. (2007). Dominant sets and pairwise clustering. *Institute of Electrical and Electronics Engineers (IEEE) Transactions on Pattern Analysis and Machine Intelligence (TPAMI)*, 29(1), 167-172.
doi:<https://doi.org/10.1109/TPAMI.2007.250608>
- Pearson, K. (1901). Liii. on lines and planes of closest fit to systems of points in space. *The London, Edinburgh, and Dublin Philosophical Magazine and Journal of Science*, 2(11), 559-572. Retrieved from <https://doi.org/10.1080/14786440109462720>
<https://arxiv.org/abs/https://doi.org/10.1080/14786440109462720>
doi:<https://doi.org/10.1080/14786440109462720>
- Piasco, N., Sidibé, D., Demonceaux, C., Gouet-Brunet, V. (2018). A survey on visual-based localization: On the benefit of heterogeneous data. *Pattern Recognition*, 74, 90-109. Retrieved from <https://www.sciencedirect.com/science/article/pii/S0031320018300000>
doi:<https://doi.org/https://doi.org/10.1016/j.patcog.2017.09.013>
- Pramanick, S., Nowara, E.M., Gleason, J., Castillo, C.D., Chellappa, R. (2022). Where in the world is this image? transformer-based geo-localization in the wild. S. Avidan, G. Brostow, M. Cissé, G.M. Farinella, & T. Hassner (Eds.), *Computer vision – eccv 2022* (pp. 196–215). Cham: Springer Nature Switzerland.
- Pumarola, A., Agudo, A., Martinez, A.M., Sanfeliu, A., Moreno-Noguer, F. (2018). Ganimation: Anatomically-aware facial animation from a single image. *Proceedings of the european conference on computer vision (eccv)* (pp. 818–833).
- Radford, A., Kim, J.W., Hallacy, C., Ramesh, A., Goh, G., Agarwal, S., ... Sutskever, I. (2021).

- Learning transferable visual models from natural language supervision. M. Meila & T. Zhang (Eds.), *Proceedings of the 38th international conference on machine learning, ICML 2021, 18-24 July 2021, virtual event* (Vol. 139, pp. 8748–8763). PMLR. Retrieved from <http://proceedings.mlr.press/v139/radford21a.html>
- Regmi, K., & Borji, A. (2018, June). Cross-view image synthesis using conditional gans. *Proceedings of the institute of electrical and electronics engineers (IEEE) conference on computer vision and pattern recognition (cvpr)*.
- Regmi, K., & Shah, M. (2019, October). Bridging the domain gap for ground-to-aerial image matching. *Proceedings of the institute of electrical and electronics engineers (IEEE)/cvf international conference on computer vision (iccv)*.
- Ren, X., Bo, L., Fox, D. (2012). Rgb-(d) scene labeling: Features and algorithms. *Institute of electrical and electronics engineers (IEEE) conference on computer vision and pattern recognition (cvpr)* (pp. 2759–2766).
- Rodrigues, R., & Tani, M. (2021, January). Are these from the same place? seeing the unseen in cross-view image geo-localization. *Proceedings of the institute of electrical and electronics engineers (IEEE)/cvf winter conference on applications of computer vision (wacv)* (p. 3753-3761).
- Roshan Zamir, A., Ardeshtir, S., Shah, M. (2014, June). Gps-tag refinement using random walks with an adaptive damping factor. *Proceedings of the institute of electrical and electronics engineers (IEEE) conference on computer vision and pattern recognition (cvpr)*.
- Santana, L.V., Brandao, A.S., Sarcinelli-Filho, M. (2015). Outdoor waypoint navigation with the ar. drone quadrotor. *International conference on unmanned aircraft systems (icuas)* (pp. 303–311).
- Saputra, M.R.U., Markham, A., Trigoni, N. (2018). Visual slam and structure from motion in dynamic environments. *ACM Computing Surveys (CSUR)*, 51, 1 - 36.
- Saurer, O., Baatz, G., Köser, K., Ladický, L., Pollefeys, M. (2015, 06). Image based geolocalization in the alps. *International Journal of Computer Vision*, 116.
- doi:<https://doi.org/10.1007/s11263-015-0830-0>
- Schroff, F., Kalenichenko, D., Philbin, J. (2015, June). Facenet: A unified embedding for face recognition and clustering. *Proceedings of the institute of electrical and electronics engineers (IEEE) conference on computer vision and pattern recognition (cvpr)*.
- Selvaraju, R.R., Cogswell, M., Das, A., Vedantam, R., Parikh, D., Batra, D. (2017, Oct). Grad-cam: Visual explanations from deep networks via gradient-based localization. *Proceedings of the institute of electrical and electronics engineers (IEEE) international conference on computer vision (iccv)*.
- Seo, P.H., Weyand, T., Sim, J., Han, B. (2018). Cplanet: Enhancing image geolocalization by combinatorial partitioning of maps. V. Ferrari, M. Hebert, C. Sminchisescu, & Y. Weiss (Eds.), *European conference on computer vision (eccv)* (pp. 544–560). Cham: Springer International Publishing.
- Shechtman, E., & Irani, M. (2007). Matching local self-similarities across images and videos. *Institute of electrical and electronics engineers (IEEE) conference on computer vision and pattern recognition (cvpr)* (p. 1-8). doi:<https://doi.org/10.1109/CVPR.2007.383198>
- Shermeyer, J., & Etten, A.V. (2019). The effects of super-resolution on object detection performance in satellite imagery. *2019 IEEE/CVF Conference on Computer Vision and Pattern Recognition Workshops (CVPRW)*, 1432-1441.
- Shi, Y., Campbell, D., Yu, X., Li, H. (2021). Geometry-guided street-view panorama synthesis from satellite imagery. *arXiv preprint arXiv:2103.01623*.

- Shi, Y., Liu, L., Yu, X., Li, H. (2019). Spatial-aware feature aggregation for image based cross-view geo-localization. *Advances in Neural Information Processing Systems (NeurIPS)*, 32, 10090–10100.
- Shi, Y., Yu, X., Campbell, D., Li, H. (2020, June). Where am i looking at? joint location and orientation estimation by cross-view matching. *Proceedings of the institute of electrical and electronics engineers (ieee)/cvf conference on computer vision and pattern recognition (cvpr)*.
- Shi, Y., Yu, X., Liu, L., Zhang, T., Li, H. (2020, Apr.). Optimal feature transport for cross-view image geo-localization. *Proceedings of the Association for the Advancement of Artificial Intelligence (AAAI) Conference on Artificial Intelligence*, 34(07), 11990-11997.
doi:<https://doi.org/10.1609/aaai.v34i07.6875>
- Shi, Y., Yu, X., Wang, S., Li, H. (2022). Cvlnet: Cross-view semantic correspondence learning for video-based camera localization. *arXiv preprint arXiv:2208.03660*.
- Shrivastava, A., Malisiewicz, T., Gupta, A., Efros, A.A. (2011). Data-driven visual similarity for cross-domain image matching. *Proceedings of the 2011 siggraph asia conference*. New York, NY, USA: Association for Computing Machinery (ACM). doi:<https://doi.org/10.1145/2024156.2024188>
- Sinkhorn, R., & Knopp, P. (1967). Concerning non-negative matrices and doubly stochastic matrices. *Pacific Journal of Mathematics*, 21(2), 343–348.
- Suenderhauf, N., Shirazi, S., Jacobson, A., Deyou, F., Pepperell, E., Upcroft, B., Milford, M. (2015). Place recognition with convnet landmarks: Viewpoint-robust, condition-robust, training-free. D. Hsu (Ed.), *Robotics: Science and systems xi* (pp. 1–10). Robotics: Science and Systems Conference.
- Tang, H., Liu, H., Xu, D., Torr, P.H., Sebe, N. (2021). Attentiongan: Unpaired image-to-image translation using attention-guided generative adversarial networks. *Institute of Electrical and Electronics Engineers (IEEE) Transactions on Neural Networks and Learning Systems (TNNLS)*.
- Tang, H., Xu, D., Sebe, N., Wang, Y., Corso, J.J., Yan, Y. (2019, June). Multi-channel attention selection gan with cascaded semantic guidance for cross-view image translation. *Proceedings of the institute of electrical and electronics engineers (ieee)/cvf conference on computer vision and pattern recognition (cvpr)*.
- Thomee, B., Shamma, D.A., Friedland, G., Elizalde, B., Ni, K., Poland, D., ... Li, L.-J. (2016, January). Yfcc100m: The new data in multimedia research. *Commun. ACM*, 59(2), 64–73.
doi:<https://doi.org/10.1145/2812802>
- Tian, Y., Chen, C., Shah, M. (2017, July). Cross-view image matching for geo-localization in urban environments. *Proceedings of the institute of electrical and electronics engineers (ieee) conference on computer vision and pattern recognition (cvpr)*.
- Toker, A., Zhou, Q., Maximov, M., Leal-Taixe, L. (2021, June). Coming down to earth: Satellite-to-street view synthesis for geo-localization. *Proceedings of the ieee/cvf conference on computer vision and pattern recognition (cvpr)* (p. 6488-6497).
- Tomešek, J., Čadík, M., Brejcha, J. (2022). Cross-locate: Cross-modal large-scale visual geo-localization in natural environments using rendered modalities. *2022 ieee/cvf winter conference on applications of computer vision (wacv)* (p. 2193-2202). doi:<https://doi.org/10.1109/WACV51458.2022.00225>
- Torii, A., Arandjelović, R., Sivic, J., Okutomi, M., Pajdla, T. (2015). 24/7 place recognition by view synthesis. *Institute of electrical and electronics engineers (ieee) conference on computer vision and pattern recognition (cvpr)* (p. 1808-1817). doi:<https://doi.org/10.1109/CVPR.2015.7298790>

- Touvron, H., Cord, M., Douze, M., Massa, F., Sablayrolles, A., Jegou, H. (2021, July). Training data-efficient image transformers distillation through attention. *International conference on machine learning* (Vol. 139, pp. 10347–10357).
- Vaswani, A., Shazeer, N., Parmar, N., Uszkoreit, J., Jones, L., Gomez, A.N., ... Polosukhin, I. (2017). Attention is all you need. I. Guyon et al. (Eds.), *Advances in neural information processing systems* (Vol. 30). Curran Associates, Inc. Retrieved from <https://proceedings.neurips.cc/paper/2017/file/3f5ee2435471ed01f5c74a847195c4a8/Paper.pdf>
- Verde, S., Resek, T., Milani, S., Rocha, A. (2020). Ground-to-aerial viewpoint localization via landmark graphs matching. *Institute of Electrical and Electronics Engineers (IEEE) Signal Processing Letters*, 27, 1490-1494.
doi:<https://doi.org/10.1109/LSP.2020.3017380>
- Vishal, K., Jawahar, C.V., Chari, V. (2015, June). Accurate localization by fusing images and gps signals. *Proceedings of the institute of electrical and electronics engineers (ieee) conference on computer vision and pattern recognition (cvpr) workshops*.
- Vo, N., & Hays, J. (2016). Localizing and orienting street views using overhead imagery. B. Leibe, J. Matas, N. Sebe, & M. Welling (Eds.), *European conference on computer vision (eccv)* (pp. 494–509). Cham: Springer International Publishing.
- Vo, N., Jacobs, N., Hays, J. (2017, Oct). Revisiting im2gps in the deep learning era. *Proceedings of the institute of electrical and electronics engineers (ieee) international conference on computer vision (iccv)*.
- Vyas, S., Chen, C., Shah, M. (2022). Gama: Cross-view video geo-localization. S. Avidan, G. Brostow, M. Cissé, G.M. Farinella, & T. Hassner (Eds.), *Computer vision – eccv 2022* (pp. 440–456). Cham: Springer Nature Switzerland.
- Wang, T., Zheng, Z., Yan, C., Zhang, J., Sun, Y., Zheng, B., Yang, Y. (2021). Each part matters: Local patterns facilitate cross-view geo-localization. *Institute of Electrical and Electronics Engineers (IEEE) Transactions on Circuits and Systems for Video Technology (TCSVT)*, 1-1.
doi:<https://doi.org/10.1109/TCSVT.2021.3061265>
- Wang, X., Yu, K., Wu, S., Gu, J., Liu, Y., Dong, C., ... Change Loy, C. (2018). Esrgan: Enhanced super-resolution generative adversarial networks. *Proceedings of the european conference on computer vision (eccv) workshops* (pp. 0–0).
- Weyand, T., Kostrikov, I., Philbin, J. (2016). Planet - photo geolocation with convolutional neural networks. B. Leibe, J. Matas, N. Sebe, & M. Welling (Eds.), *European conference on computer vision (eccv)* (pp. 37–55). Cham: Springer International Publishing.
- Wilson, D., Alshaabi, T., Oort, C.M.V., Zhang, X., Nelson, J., Wshah, S. (2021). Object tracking and geo-localization from street images. *CoRR*, [abs/2107.06257](https://arxiv.org/abs/2107.06257).
- Woo, S., Park, J., Lee, J.-Y., Kweon, I.S. (2018, September). Cbam: Convolutional block attention module. *Proceedings of the european conference on computer vision (eccv)*.
- Workman, S., Souvenir, R., Jacobs, N. (2015, December). Wide-area image geolocation with aerial reference imagery. *Proceedings of the institute of electrical and electronics engineers (ieee) international conference on computer vision (iccv)*.
- Xia, G.-S., Bai, X., Ding, J., Zhu, Z., Belongie, S., Luo, J., ... Zhang, L. (2018). Dota: A large-scale dataset for object detection in aerial images. *Proceedings of the institute of electrical and electronics engineers (ieee) conference on computer vision and pattern recognition (cvpr)* (pp. 3974–3983).
- Xia, H., Zhao, H., Ding, Z. (2021, October). Adaptive adversarial network for source-free domain

- adaptation. *Proceedings of the IEEE/CVF International Conference on Computer Vision (ICCV)* (p. 9010-9019).
- Xiao, J., Hays, J., Ehinger, K.A., Oliva, A., Torralba, A. (2010). Sun database: Large-scale scene recognition from abbey to zoo. *Institute of Electrical and Electronics Engineers (IEEE) Computer Society Conference on Computer Vision and Pattern Recognition (CVPR)* (p. 3485-3492). doi:<https://doi.org/10.1109/CVPR.2010.5539970>
- Yi, Z., Zhang, H., Tan, P., Gong, M. (2017, Oct). Dual-gan: Unsupervised dual learning for image-to-image translation. *Proceedings of the Institute of Electrical and Electronics Engineers (IEEE) International Conference on Computer Vision (ICCV)*.
- You, K., Long, M., Cao, Z., Wang, J., Jordan, M.I. (2019, June). Universal domain adaptation. *Proceedings of the IEEE/CVF Conference on Computer Vision and Pattern Recognition (CVPR)*.
- Zamir, A.R., & Shah, M. (2010). Accurate image localization based on google maps street view. K. Daniilidis, P. Maragos, & N. Paragios (Eds.), *European Conference on Computer Vision (ECCV)* (pp. 255–268). Berlin, Heidelberg: Springer Berlin Heidelberg.
- Zamir, A.R., & Shah, M. (2014). Image geo-localization based on multiple nearest neighbor feature matching using generalized graphs. *Institute of Electrical and Electronics Engineers (IEEE) Transactions on Pattern Analysis and Machine Intelligence (TPAMI)*, 36(8), 1546-1558.
doi:<https://doi.org/10.1109/TPAMI.2014.2299799>
- Zhai, M., Bessinger, Z., Workman, S., Jacobs, N. (2017, July). Predicting ground-level scene layout from aerial imagery. *Proceedings of the IEEE Conference on Computer Vision and Pattern Recognition (CVPR)*.
- Zhang, H., Berg, A., Maire, M., Malik, J. (2006). Svm-knn: Discriminative nearest neighbor classification for visual category recognition. *Institute of Electrical and Electronics Engineers (IEEE) Computer Society Conference on Computer Vision and Pattern Recognition (CVPR)* (Vol. 2, p. 2126-2136). doi:<https://doi.org/10.1109/CVPR.2006.301>
- Zhang, X., Li, X., Sultani, W., Zhou, Y., Wshah, S. (2023, Jun.). Cross-view geo-localization via learning disentangled geometric layout correspondence. *Proceedings of the AAAI Conference on Artificial Intelligence*, 37(3), 3480-3488. Retrieved from <https://ojs.aaai.org/index.php/AAAI/article/view/25457>
doi:<https://doi.org/10.1609/aaai.v37i3.25457>
- Zhang, X., Sultani, W., Wshah, S. (2023, January). Cross-view image sequence geo-localization. *Proceedings of the IEEE/CVF Winter Conference on Applications of Computer Vision (WACV)* (p. 2914-2923).
- Zheng, L., Yang, Y., Tian, Q. (2016, 08). Sift meets cnn: A decade survey of instance retrieval. *IEEE Transactions on Pattern Analysis and Machine Intelligence, PP*.
doi:<https://doi.org/10.1109/TPAMI.2017.2709749>
- Zheng, Z., Wei, Y., Yang, Y. (2020). University-1652: A multi-view multi-source benchmark for drone-based geo-localization. *Proceedings of the 28th ACM International Conference on Multimedia* (p. 1395–1403). New York, NY, USA: Association for Computing Machinery. doi:<https://doi.org/10.1145/3394171.3413896>
- Zhou, B., Lapedriza, A., Xiao, J., Torralba, A., Oliva, A. (2014). Learning deep features for scene recognition using places database. Z. Ghahramani, M. Welling, C. Cortes, N. Lawrence, & K.Q. Weinberger (Eds.), *Advances in Neural Information Processing Systems (NeurIPS)* (Vol. 27). Curran Associates, Inc.
- Zhou, B., Liu, L., Oliva, A., Torralba, A. (2014). Recognizing city identity via attribute analysis of geo-tagged images. D. Fleet, T. Pajdla, B. Schiele, & T. Tuytelaars (Eds.), *European*

conference on computer vision (eccv) (pp. 519–534). Cham: Springer International Publishing.

- Zhu, J.-Y., Park, T., Isola, P., Efros, A.A. (2017, Oct). Unpaired image-to-image translation using cycle-consistent adversarial networks. *Proceedings of the institute of electrical and electronics engineers (ieee) international conference on computer vision (iccv)*.
- Zhu, J.-Y., Zhang, R., Pathak, D., Darrell, T., Efros, A.A., Wang, O., Shechtman, E. (2017). Toward multimodal image-to-image translation. I. Guyon et al. (Eds.), *Advances in neural information processing systems 30* (pp. 465–476). Curran Associates, Inc.
- Zhu, S., Shah, M., Chen, C. (2022, June). Trans-geo: Transformer is all you need for cross-view image geo-localization. *Proceedings of the ieee/cvf conference on computer vision and pattern recognition (cvpr)* (p. 1162-1171).
- Zhu, S., Yang, T., Chen, C. (2021a, January). Revisiting street-to-aerial view image geo-localization and orientation estimation. *Proceedings of the institute of electrical and electronics engineers (ieee)/cvf winter conference on applications of computer vision (wacv)* (p. 756-765).
- Zhu, S., Yang, T., Chen, C. (2021b, June). Vigor: Cross-view image geo-localization beyond one-to-one retrieval. *Proceedings of the ieee/cvf conference on computer vision and pattern recognition (cvpr)* (p. 3640-3649).